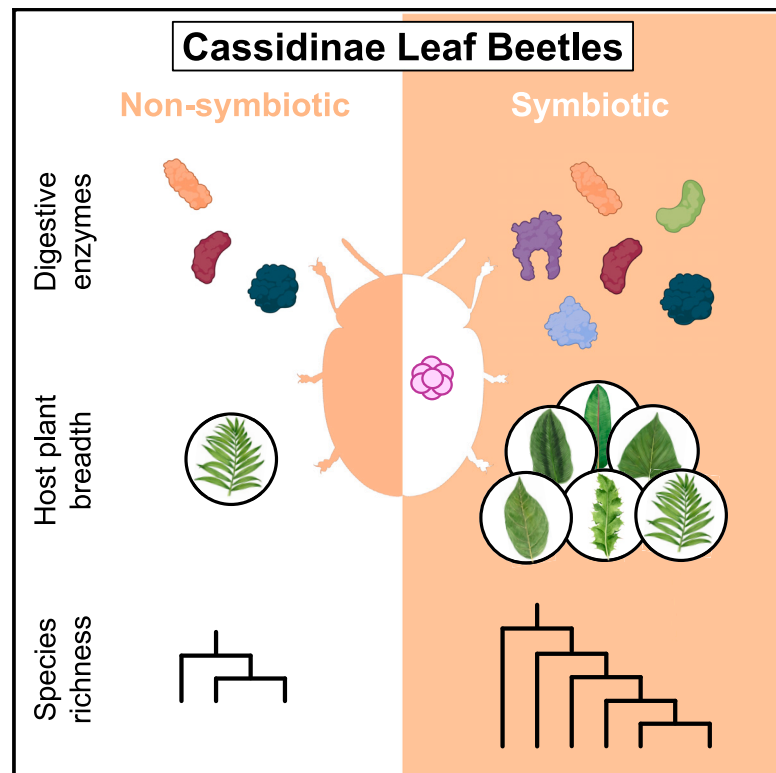


Current Biology

Paleocene origin of a streamlined digestive symbiosis in leaf beetles

Graphical abstract



Authors

Marleny García-Lozano,
Christine Henzler,
Miguel Ángel González Porras, ...,
Takema Fukatsu, Donald Windsor,
Hassan Salem

Correspondence

hassan.salem@tuebingen.mpg.de

In brief

García-Lozano et al. time the acquisition and quantify the adaptive impact of a digestive symbiosis between leaf beetles and *Stammera*, a bacterium. Compared with their non-symbiotic relatives, *Stammera*-harboring leaf beetles deploy a greater variety of digestive enzymes, exploit a broader range of plants, and are more speciose.

Highlights

- *Stammera* is a shared symbiont across tortoise and hispine leaf beetles
- *Stammera* modulates its transcriptional profile to match host requirements
- The digestive symbiosis originated in the Paleocene (62 mya)
- Symbiotic beetles are more speciose than their non-symbiotic relatives

Article

Paleocene origin of a streamlined digestive symbiosis in leaf beetles

Marleny García-Lozano,¹ Christine Henzler,¹ Miguel Ángel González Porras,¹ Inès Pons,¹ Aileen Berasategui,^{1,2} Christa Lanz,³ Heike Budde,⁴ Kohei Oguchi,^{5,6} Yu Matsuura,⁷ Yannick Pauchet,⁸ Shana Goffredi,⁹ Takema Fukatsu,⁵ Donald Windsor,¹⁰ and Hassan Salem^{1,10,11,*}

¹Mutualisms Research Group, Max Planck Institute for Biology, Tübingen 72076, Germany

²Amsterdam Institute for Life and Environment, Vrije Universiteit, Amsterdam 1081 HV, the Netherlands

³Genome Center, Max Planck Institute for Biology, Tübingen 72076, Germany

⁴Department of Microbiome Science, Max Planck Institute for Biology, Tübingen 72076, Germany

⁵National Institute for Advanced Industrial Science and Technology, Tsukuba 305-8566, Japan

⁶Misaki Marine Biological Station, The University of Tokyo, Miura 238-0225, Japan

⁷Tropical Biosphere Research Center, University of the Ryukyus, Okinawa 903-0213, Japan

⁸Department of Insect Symbiosis, Max Planck Institute for Chemical Ecology, Jena 07745, Germany

⁹Department of Biology, Occidental College, Los Angeles, CA 90041, USA

¹⁰Smithsonian Tropical Research Institute, Panama City 0843-03092, Panama

¹¹Lead contact

*Correspondence: hassan.salem@tuebingen.mpg.de

<https://doi.org/10.1016/j.cub.2024.01.070>

SUMMARY

Timing the acquisition of a beneficial microbe relative to the evolutionary history of its host can shed light on the adaptive impact of a partnership. Here, we investigated the onset and molecular evolution of an obligate symbiosis between Cassidinae leaf beetles and *Candidatus Stammera capleta*, a γ -proteobacterium. Residing extracellularly within foregut symbiotic organs, *Stammera* upgrades the digestive physiology of its host by supplementing plant cell wall-degrading enzymes. We observe that *Stammera* is a shared symbiont across tortoise and hispine beetles that collectively comprise the Cassidinae subfamily, despite differences in their folivorous habits. In contrast to its transcriptional profile during vertical transmission, *Stammera* elevates the expression of genes encoding digestive enzymes while in the foregut symbiotic organs, matching the nutritional requirements of its host. Despite the widespread distribution of *Stammera* across Cassidinae beetles, symbiont acquisition during the Paleocene (~62 mya) did not coincide with the origin of the subfamily. Early diverging lineages lack the symbiont and the specialized organs that house it. Reconstructing the ancestral state of host-beneficial factors revealed that *Stammera* encoded three digestive enzymes at the onset of symbiosis, including polygalacturonase—a pectinase that is universally shared. Although non-symbiotic cassidines encode polygalacturonase endogenously, their repertoire of plant cell wall-degrading enzymes is more limited compared with symbiotic beetles supplemented with digestive enzymes from *Stammera*. Highlighting the potential impact of a symbiotic condition and an upgraded metabolic potential, *Stammera*-harboring beetles exploit a greater variety of plants and are more speciose compared with non-symbiotic members of the Cassidinae.

INTRODUCTION

Folivores must contend with a diet rich in recalcitrant plant polymers such as cellulose and pectin.¹ Tortoise beetles (Chrysomelidae: Cassidinae) overcome these challenges by encoding cellulases endogenously² while outsourcing their pectinolytic metabolism to *Candidatus Stammera capleta*, a γ -proteobacterial symbiont.^{3–8}

Tortoise beetles house *Stammera* extracellularly in foregut symbiotic organs, in addition to ovary-associated glands to ensure transmission.^{3,5,6} Encoded within the symbiont's drastically reduced genome (0.21 Mb) are plant cell wall-degrading enzymes that upgrade the digestive ability of the beetle host.^{3,4,8} Females vertically propagate the symbiosis by

depositing a *Stammera*-bearing “caplet” at the anterior pole of each egg.^{3,5,7} As caplet consumption initiates infection by *Stammera* during embryo development,⁹ its experimental removal disrupts the symbiont's transmission cycle, yielding aposymbiotic insects.^{3,7} The prehatch acquisition of *Stammera* is unique relative to extracellularly transmitted symbionts,^{7,9} which are typically integrated during early instar stages such as larvae and nymphs,¹⁰ as demonstrated in bugs,^{11–14} bees,¹⁵ and ants.¹⁶ Among tortoise beetles, symbiont loss results in a diminished digestive capacity and low larval survivorship,^{3,7} highlighting an obligate dependence on *Stammera*.

The Cassidinae represents a highly diverse subfamily of leaf beetles, with more than 6,000 herbivorous species occupying a variety of ecological guilds.¹⁷ The monophyletic group includes

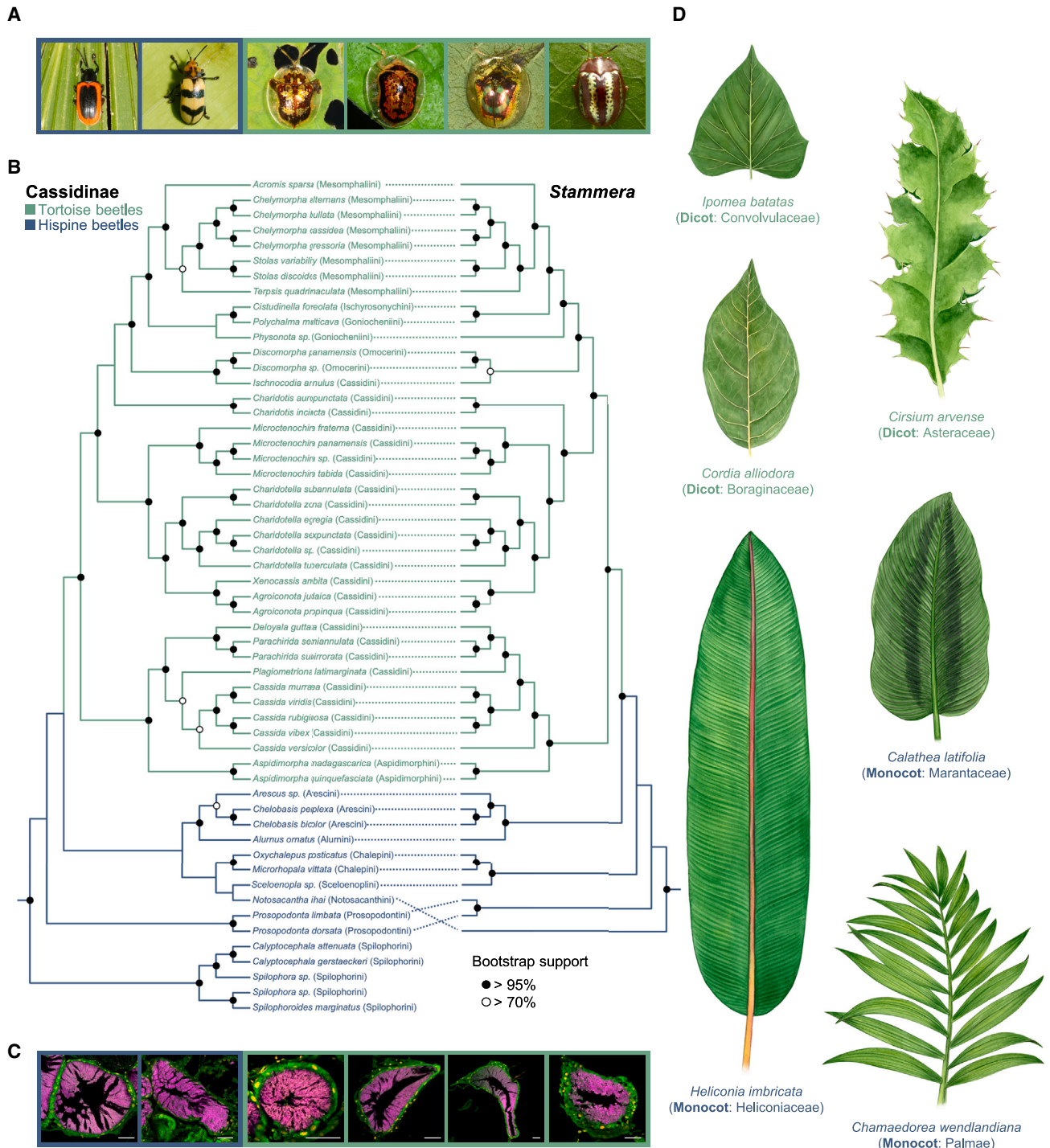


Figure 1. *Stammera* is a shared symbiont across tortoise and hispine beetles

(A) Hispine (blue outlines) and tortoise beetles (green outlines) from left to right: *Prosopodonta limbata*, *Chelobasis bicolor*, *Deloyala guttata*, *Microctenochira tabida*, *Charidotella zona*, and *Chelymorpha alternans*.

(B) Tanglegram depicting co-cladogenesis between Cassidinae beetles and their *Stammera* symbionts based on maximum likelihood (ML) phylogenies. Host tribes are indicated in parentheses. The Cassidinae phylogeny is based on a concatenated alignment of 15 mitochondrial genes, whereas the *Stammera* phylogeny was constructed using a concatenated alignment of 61 single-copy core genes. Node coloration reflects bootstrap support. Detailed ML phylogenies, including outgroups along with their complementary Bayesian phylogenetic trees for host and symbiont, are included in [Figures S1](#) and [S2](#).

(legend continued on next page)

exophagous tortoise beetles, along with hispine beetles that are largely leaf-mining and were formerly classified as a separate subfamily (Chrysomelidae: Hispinae) (Figures 1A and 1B).^{17–19} A suite of morphological and behavioral traits differentiates both groups,¹⁷ but, critically, tortoise beetles vary from hispines in their host-plant use.^{18–20} Hispines feed predominantly on monocotyledonous plants such as grasses and palms, whereas tortoise beetles coevolved with a dicotyledonous flora,¹⁷ reflecting a derived dietary shift that corresponded with the emergence and diversification of a then-novel niche during the Cretaceous.^{21,22}

Previous efforts characterizing the Cassidinae-*Stammera* symbiosis focused exclusively on dicot-feeding taxa, suggesting that the partnership may have originated with, and is restricted to, tortoise beetles.^{3,4,6} Given their divergent nutritional ecology, it remained unclear whether tortoise and hispine beetles are both hosts to *Stammera*,^{4,6,23} despite their shared ancestry.¹⁷ Notably, if symbiont acquisition did not coincide with the origin of the subfamily, how do non-symbiotic cassidines process a leafy diet in the absence of *Stammera*-encoded pectinases?

Here, we determine the origin of the Cassidinae-*Stammera* symbiosis and emphasize the divergent strategies facilitating a folivorous lifestyle across a highly speciose clade of beetles. We do so by (1) reconstructing host-symbiont phylogenetic relationships spanning a wider and more representative distribution of Cassidinae tribes, including hispine lineages, (2) assessing the *Stammera* pangenome across 50 species to examine patterns of molecular evolution and testing for signatures of selection, (3) reconstructing the ancestral configuration of host-beneficial factors, (4) quantifying the symbiont's transcriptional dynamics relative to beetle development and nutritional requirements, and (5) timing the acquisition of *Stammera* and estimating its potential impact on the diversification of its herbivorous host.

RESULTS AND DISCUSSION

Stammera is a shared symbiont across tortoise and hispine beetles

Initial descriptions of the *Stammera*-Cassidinae symbiosis examined five tortoise beetle tribes.^{3,4,6} Here, we extended our characterization of the partnership to 13 tribes (totaling 55 species) (Figures 1A–1D), emphasizing hispine clades considered to represent early diverging Cassidinae lineages, including the Alurnini and Spilophorini.¹⁷

Metagenomic sequencing revealed the presence of *Stammera* in both tortoise and hispine beetles. Of the 55 Cassidinae species examined here, 50 are hosts to *Stammera* (Figure 1B). This is complemented by the presence of morphologically conserved symbiotic organs in hispines relative to the *Stammera*-bearing structures previously described in tortoise beetles (Figure 1C).^{3,5,6} Both groups maintain *Stammera* extracellularly in specialized symbiotic organs connected to the foregut-midgut junction (Figure 1C). Reflecting the maternal inheritance of

Stammera,^{3,7} we observe near-strict co-cladogenesis between the Cassidinae and their symbionts (Figure 1B) highlighted by 40 co-speciation events relative to 9 potential transfers across host lineages. This is consistent with insect symbionts that are transmitted vertically,¹⁰ as demonstrated in aphids,²⁴ cicadas,²⁵ stinkbugs,²⁶ and bat flies.²⁷

Although most hispine beetles surveyed in our study do harbor *Stammera* (Figures 1A–1C), members of the earliest-diverging Spilophorini tribe lack the symbiont (Figure 1B) and the corresponding *Stammera*-bearing organs. But although *Stammera* acquisition did not coincide with the origin of the Cassidinae, the digestive symbiosis predated the obligate monocot-to-dicot evolutionary transition that is concomitant with the rise and subsequent diversification of tortoise beetles (Figures 1B and 1D).

A comparative analysis spanning 50 *Stammera* genomes revealed that their sizes are drastically and consistently reduced, ranging from 216 to 340 kb, and bearing only 201–317 protein-coding genes. Both parameters are positively correlated (Spearman's rank correlation, $\rho = 0.934$, $p < 0.001$) (Data S1) as observed in other bacterial genomes,²⁸ including insect symbionts.²⁹ We also note that *Stammera* associating with tortoise beetles possess the smallest genomes, in contrast to symbionts characterized in hispines (Data S1), which possess the largest. In addition to a single chromosome, most *Stammera* strains carry 1–2 plasmids ranging in size between 2.5 and 9 kb. Although plasmids predominantly encode the host-beneficial factors supplemented by *Stammera*, we observe the loss of these extra-chromosomal elements in a subset of species (e.g., *Stammera* from *Terpsis quadrimaculata*), followed by their integration into the symbiont chromosome.

To characterize how *Stammera* metabolic potential compares across hispine and tortoise beetles, we examined shared orthologues and gene loss following a pangenome analysis as implemented in *anvi'o*.³⁰ Our analysis revealed a pangenome composed of 503 gene clusters, of which 125 (24.9%) are shared by all *Stammera* strains (core genes) (Data S2A), compared with the 295 (58.6%) clusters representing the accessory gene set (Data S2B) and 83 (16.5%) singletons (Data S2C) (Figure 2). Categories related to basic informational processes (replication, transcription, and translation) and posttranslational modification are highly represented within the core genome, whereas gene clusters underlying energy production, metabolism, and cell wall biogenesis are prevalent in the accessory genome (Figure S3). Such variance is observed in *Stammera* with the smallest genomes, suggesting that gene loss, rather than acquisition and rearrangement, might drive these differences, as recombination is expected to be minimal in clonal populations of vertically transmitted symbionts.²⁴ Although 315 orthologous genes are shared between *Stammera* from tortoise and hispine beetles, a large proportion of genes are also uniquely present in each group (71 and 117, respectively) (Figure 3A). Upon comparing the Clusters of Orthologous Groups (COG) annotations across both groups, we identified pathways that are statistically enriched in *Stammera* genomes from hispine beetles. These

(C) Fluorescence *in situ* hybridization (FISH) cross-sections of foregut symbiotic organs of the Cassidinae beetle species outlined above, targeting *Stammera* (magenta: 16 rRNA) and host (green: 18 rRNA) cells against the DAPI counterstain (yellow). Scale bars (50 μm) are included for reference.

(D) Illustrations portraying representative host plants of hispine (monocots: *Chamaedorea wendlandiana*, *Heliconia imbricata*, and *Calathea latifolia*) and tortoise beetles (dicots: *Cordia alliodora*, *Cirsium arvense*, and *Ipomoea batatas*).

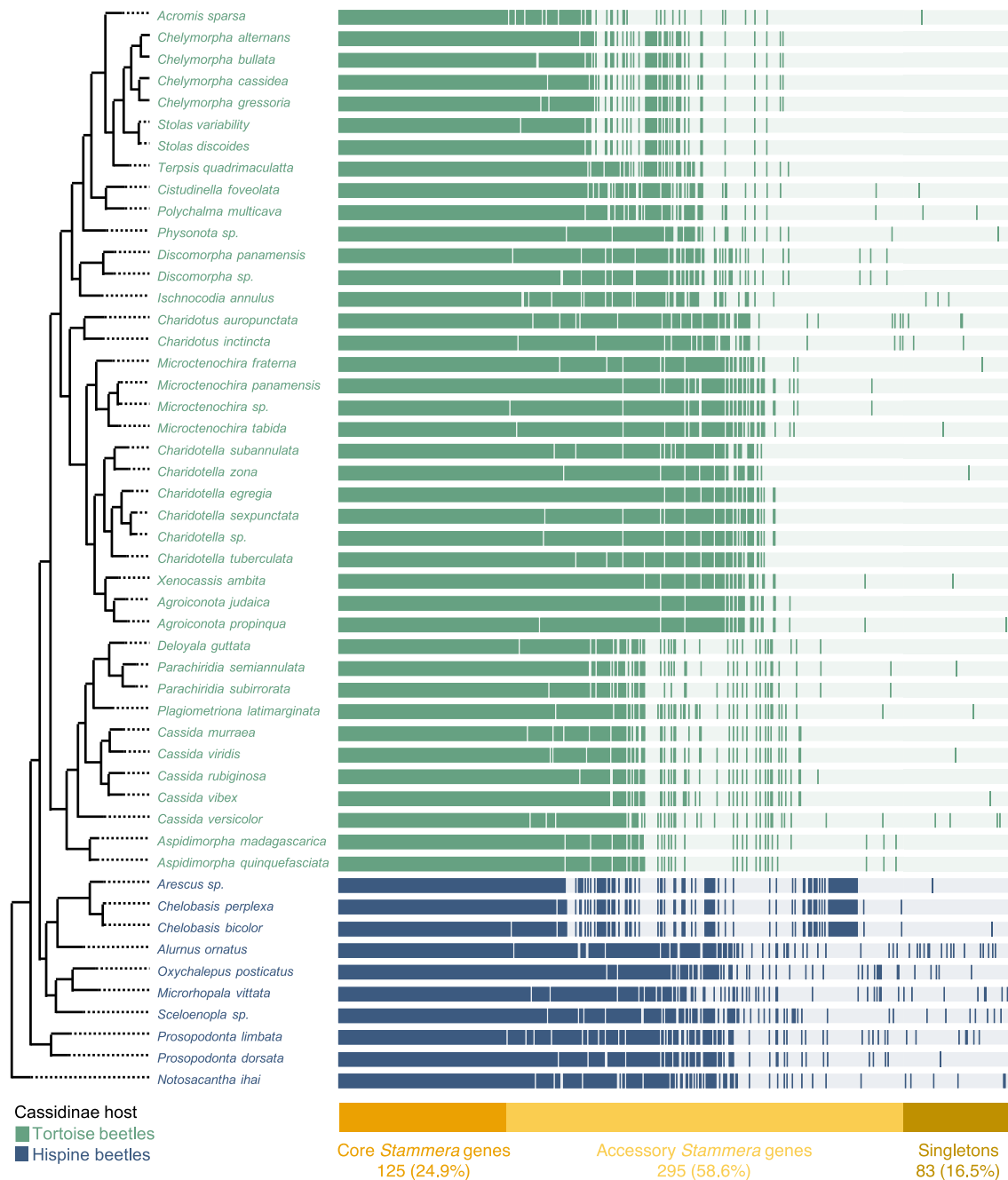


Figure 2. Core and accessory genes across the *Stammera* pangenome

Comparative genomics of 50 *Stammera* strains depicting the distribution of core, accessory, and singleton genes. Each bar represents a *Stammera* genome from one Cassidinae host, and each layer illustrates the presence or absence of a gene cluster across the different genomes. Genomes are ordered according to a maximum likelihood *Stammera* phylogeny constructed using 124 single-copy core genes. Core genes indicate gene clusters identified in all genomes, and accessory genes represent gene clusters discretely distributed but present in at least one genome. Singletons are genes present in only one genome. Coloration differentiates *Stammera* from tortoise (green) and hispine (blue) beetles.

See also [Figure S3](#) and [Data S1](#), [S2](#), and [S3](#).

pathways included lipoate biosynthesis (q value < 0.01), pyruvate oxidation (q value < 0.01), isoleucine, leucine, valine biosynthesis (q value < 0.05), and menaquinone biosynthesis (q value < 0.05). By contrast, no pathways were statistically enriched in *Stammera* genomes from tortoise beetles.

Such findings are consistent with the metabolic streamlining observed in *Stammera* and other insect endosymbionts,^{24,31,32} where in the absence of opportunities for recombination, gene loss is unidirectional. Finally, by examining gene order across representative symbiont genomes spanning the Cassidinae,

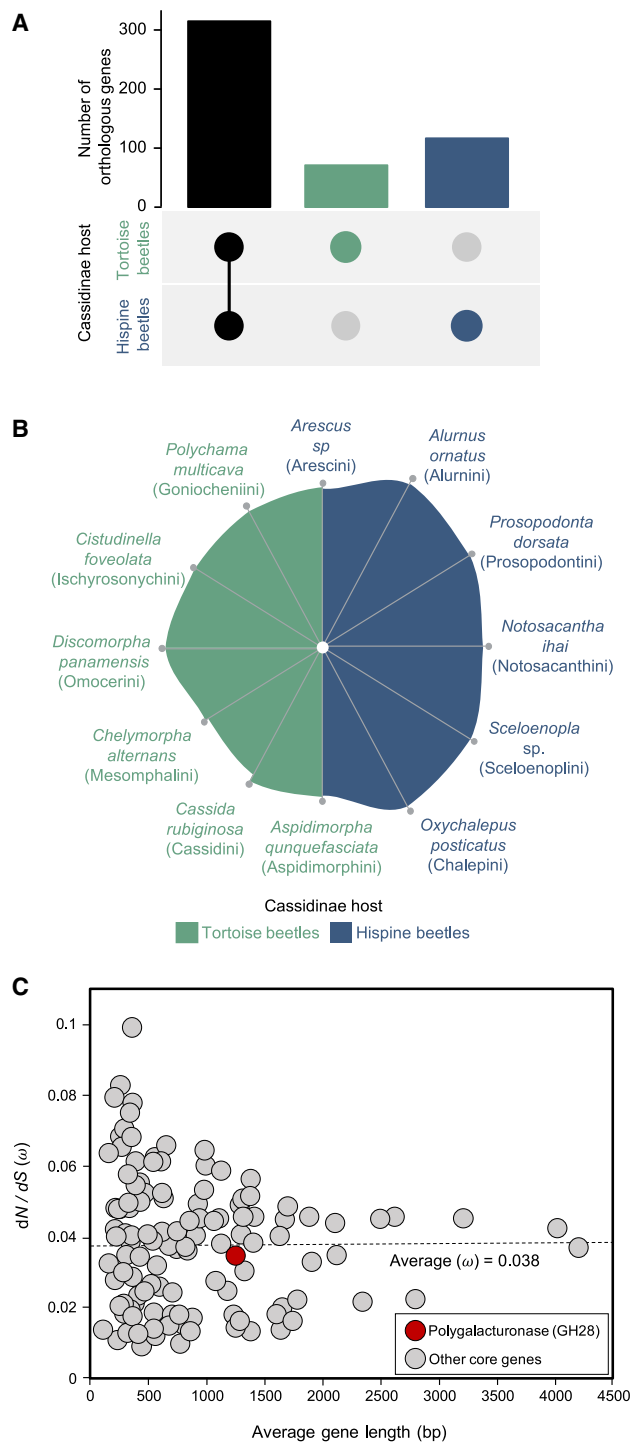


Figure 3. *Stammera* genomic features and molecular evolution
(A) UpSet plot of shared and non-shared gene content between *Stammera* from tortoise (green) and hispine beetles (blue).
(B) Hive plot depicting gene order conservation spanning representative *Stammera* strains across the 12 Cassidinae host tribes surveyed in this study. *Stammera* genome sequences are represented by nodes placed on radial axes, and conserved genomic regions are linked through connecting ribbons. The scales for the radial axes represent the genome size of each *Stammera* strain.
(C) Relationship between average gene length and nonsynonymous (dN) to synonymous (dS) substitution values for core genes (gray), including

we note that *Stammera* chromosomes are highly syntenic (Figure 3B). The high level of synteny, coupled with the monophyly of *Stammera* within the Enterobacteriaceae (Figures 1B and S1), point to a single origin of symbiosis with the Cassidinae.

Stammera genes experiencing purifying selection

Genome-wide tests for selection can help identify genes underlying co-adaptation between a symbiont and its host.^{24,33,34} For example, by estimating the rate (ω) of nonsynonymous (dN) to synonymous (dS) substitutions acting on *Buchnera* genes, Chong and Moran²⁴ revealed a small subset of loci undergoing positive selection ($\omega > 1$). These featured *Buchnera* membrane proteins that are highly expressed within the symbiotic organs of aphids,³⁵ possibly facilitating interactions at the host-symbiont interface.²⁴ By contrast, purifying selection ($\omega < 0.1$) plays key role in preserving the functionality of long-term partnerships by purging deleterious mutations impacting critical functions, as highlighted for the obligate symbionts of leafhoppers,³³ cicadas,³⁶ and earthworms.³⁷

We leveraged the 50 *Stammera* genomes available in our study to examine the signatures of selection acting on shared loci by estimating ω across whole genes. Using the M0 model as implemented in PAML,³⁸ this initial estimate revealed that *Stammera* genomes are experiencing strong purifying selection (average $\omega = 0.038$, [range = 0.008–0.098, n = 124]). By contrast, we observe no support for relaxed ($0.95 < \omega > 0.1$) or positive selection ($\omega > 1$). As specific codons related to intrinsic protein function may be experiencing different signatures relative to the whole gene, we additionally measured ω across codon sites and compared the site-based models M1a (nearly neutral) and M2a (positive selection). ω values were indicative of relaxed purifying selection (average $\omega = 0.119$), revealing the absence of any positively selected sites within orthologous *Stammera* genes.

Strong selective constraints are described across several symbiont lineages, preserving key cellular functions, along with biosynthetic pathways that are essential for host development.³⁴ Purifying selection is critical for the stability of obligately co-dependent partnerships and a driver of genome evolution across endosymbionts such as *Blattabacterium* in cockroaches³⁹ and *Thiodiazotropha* in clams,⁴⁰ as well as beneficial extracellular microbes such as *Verminephrobacter* in earthworms.³⁷ Gene categories underlying informational processing, chaperones, and host-beneficial factors typically exhibit the strongest levels of purifying selection.⁴¹ We observe that many of these genes are evolving under similar selective constraints in *Stammera* (Figure 3C; Data S3). Of the 20 *Stammera* genes exhibiting the lowest ω values (0.009–0.018), 17 are involved in transcription, translation, and replication (e.g., *rho*, *infA*, and *polA*), two underlie post-translational modification (e.g., *smgB* and *rsmD*), and one is involved in amino acid transport and metabolism (e.g., *sufS*) (Data S3). Symbiont pathways encoding key metabolites for the host can experience similar selective pressures, including *Buchnera* genes involved in amino acid biosynthesis for aphids, or the

polygalacturonase (red), a pectinase. Average gene length was calculated across all *Stammera* species. Dashed line represents the average rate (ω) of dN/dS substitutions across orthologous symbiont genes. Abbreviation is as follows: GH, glycoside hydrolase. See also Data S1, S2, and S3.

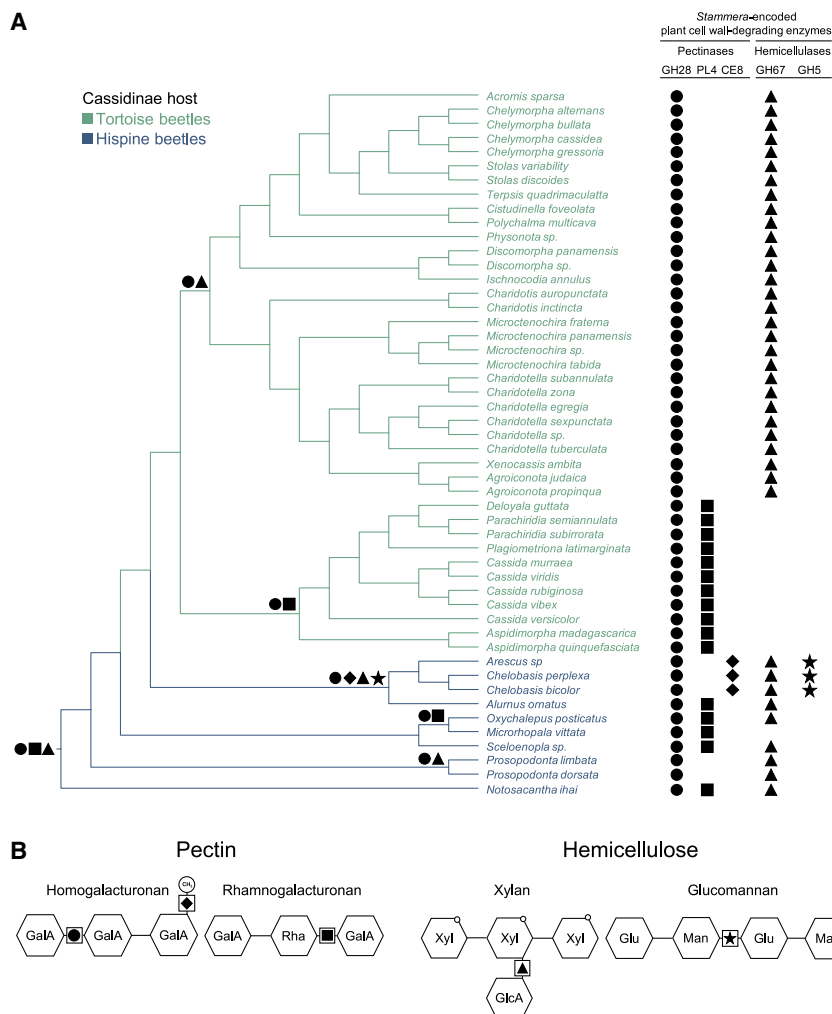


Figure 4. Distribution and ancestral reconstruction of *Stammera*-encoded digestive enzymes

(A) Distribution of *Stammera* genes encoding plant cell wall-degrading enzymes is represented by different symbols. Circle, GH28 (polygalacturonase); rectangle, PL4 (rhamnogalacturonan lyase); diamond, CE8 (pectin methylesterase); triangle, GH67 (α -glucuronidase), and star, GH5 (mannanase). Symbiont maximum likelihood phylogeny is based on a concatenated alignment of 124 single-copy core genes. The ancestral state of host-beneficial factors was inferred using the trace character history function as implemented in Mesquite v3.7. A character matrix was created for all genes, and likelihood calculations were performed using the Mk1 model. A likelihood score > 50% was used to infer ancestral nodes for the different plant cell wall-degrading enzymes encoded by *Stammera* and are illustrated by symbols at the base of each node.

(B) Predicted mode of action of *Stammera* digestive enzymes across pectin and hemicellulose. Abbreviations are as follows: GH, glycoside hydrolase; GlcA, glucuronic acid; Glu, glucose; CE, carbohydrate esterase; Man, mannose; PL, polysaccharide lyase; Rha, rhamnose; and Xyl, xylose.

enzymes, including a pectin methylesterase (carbohydrate esterase [CE] 8) and a mannanase (GH5), both of which are restricted to hispine symbionts (Figure 4).

Using the trace character history function as implemented in Mesquite,⁴² we reconstructed the distribution of symbiont-encoded digestive enzymes relative to the evolutionary history of *Stammera* (Figure 4).

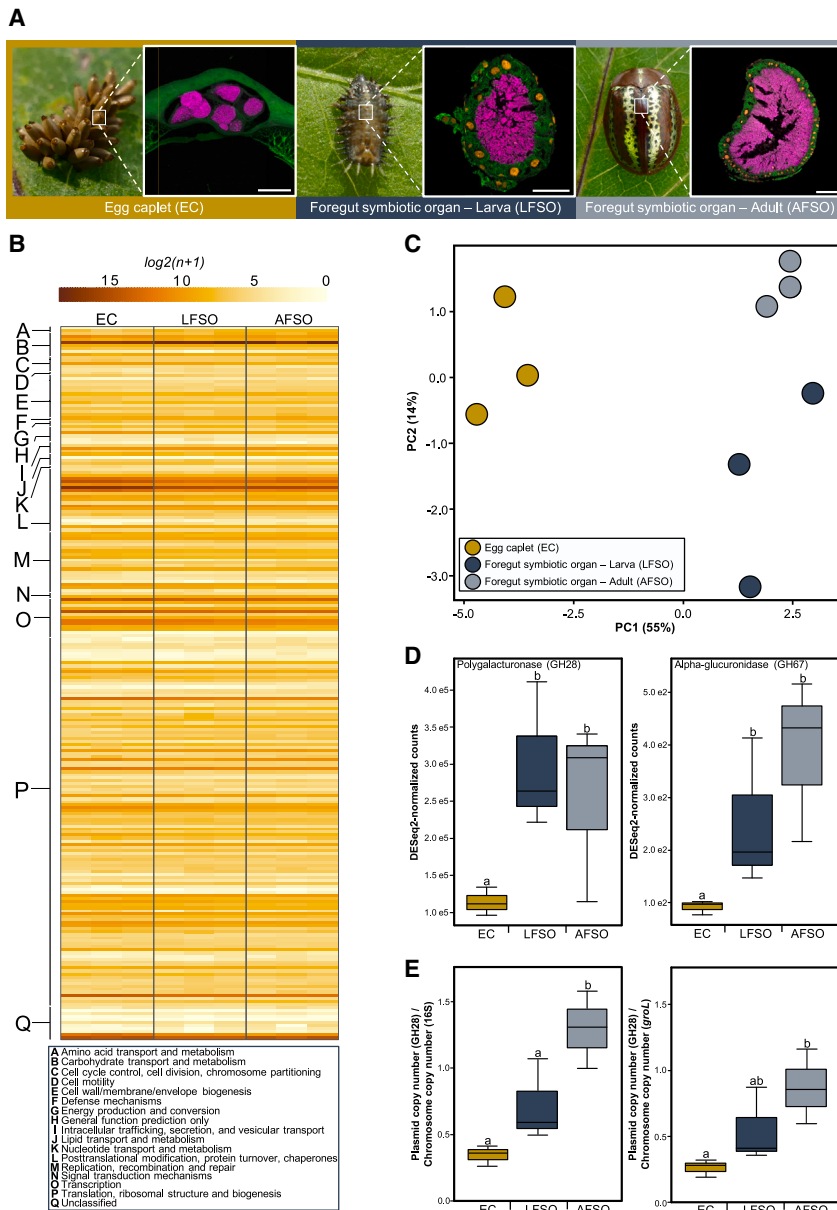
nitrogen metabolism of *Blochmannia* in ants and *Wigglesworthia* in tsetse flies.³⁹ We examined the signature of selection acting on polygalacturonase (Figure 3C)—a pectinase targeting nature’s most abundant pectic substrate, homogalacturonan—and the sole host-beneficial factor shared by all *Stammera* strains surveyed here (Figure 4). We observe that the pectinase is more constrained in its evolutionary change ($\omega = 0.035$) than the average of all core genes (Figure 3C; Data S3), reflecting its role in underpinning this digestive symbiosis in Cassidinae beetles.

Ancestral configuration of host-beneficial factors

As the *Stammera*-Cassidinae symbiosis is predicated on the microbe’s ability to deconstruct complex plant polymers,^{3,4} we assessed the distribution, assembly, and ancestral configuration of the symbiont’s plant cell wall-degrading enzymes. Our annotation of *Stammera* genomes spanning tortoise and hispine beetles yielded a diversity of digestive enzymes, matching the divergent nutritional ecology of cassidines (Figure 4). These feature previously described pectinases such as polygalacturonase (glycoside hydrolase [GH] 28) and rhamnogalacturonan lyase (polysaccharide lyase [PL] 4), together with α -glucuronidase (GH67), a xylanase.^{3,4,8} However, our examination of the partnership beyond tortoise beetles revealed additional *Stammera*-encoded digestive

We observe that the ancestral configuration of the symbiosis featured three plant cell wall-degrading enzymes: polygalacturonase (GH28), α -glucuronidase (GH67), and rhamnogalacturonan lyase (PL4) (Figure 4A). Although pectin methylesterase and mannanase were acquired secondarily, we find that gene loss, rather than gain or reacquisition, generally govern the presence of host-beneficial factors (Figure 4A). Except for polygalacturonase, which is encoded by all *Stammera* strains surveyed to date (Figure 4A), at least four irreversible loss events shaped the distribution of the remaining digestive enzymes (Figure 4A).

Among hispines, the annotation of mannanases in *Stammera* is notable given the predominant specialization of these beetles on monocotyledonous plants.¹⁷ Monocots represent an especially rich source of glucomannan,^{43,44} and mannanases can deconstruct the hemicellulose by cleaving its β -1,4-linkage of glucose and mannose⁴⁵ (Figure 4B). As mannanases are not encoded by *Stammera* in tortoise beetles (Figure 4A), their restriction to symbionts associated with hispines may reflect the adaptation of cassidines to monocotyledonous plants,¹⁷ including palms and grasses (Figure 1D). Thus, we predicted that *Stammera* may differentially upgrade the digestive physiology in a subset of hispines relative to tortoise beetles, allowing them to exploit a diet rich in glucomannan. Using thin-layer chromatography,



we compared the digestive phenotype of a hispine (*Chelobasis bicolor*) and a tortoise beetle (*Chelymorpha alternans*) bearing metabolically distinct symbionts (Figure S4). Since both species harbor *Stammera* capable of supplementing polygalacturonase, we observe that the two beetles can monomerize homogalacturonan into galacturonic acid (Figure S4A). But confirming *in silico* predictions that *C. bicolor* should depolymerize glucomannan more effectively (owing to its symbiont encoding a mannanase), we find that the hispine is able to deconstruct the hemicellulose into pronounced dimers and trimers, compared with the breakdown products accumulating in *C. alternans* (Figure S4B).

Symbiont transcriptional variation matches host nutritional requirements

Characterizing the transcriptional activity of *Stammera* in foregut symbiotic organs of adult beetles revealed a consistent profile

Figure 5. *Stammera* transcriptional dynamics match host nutritional requirements

(A) *Chelymorpha alternans* eggs, larva (3rd instar), and adult. Fluorescence *in situ* hybridization using cross-sections of egg caplets and foregut symbiotic organs of a larva and an adult targeting *Stammera* (magenta: 16 rRNA) and host (green: 18 rRNA) cells against the DAPI counterstain (yellow). Scale bars (50 μ m) are included for reference.

(B) Heatmap illustrating *Stammera* gene expression across egg caplets and foregut symbiotic organs in larvae and adults.

(C) Principal coordinate analysis (PCA) of the global transcriptome profile of *Stammera* across host compartments. Significant clustering was assessed by PERMANOVA based on Euclidean distances between samples ($p = 0.003$).

(D) Expression of polygalacturonase (left) and α -glucuronidase (right) genes of *Stammera* across host compartments. Counts were normalized by DESeq2's median of ratios. Differences in gene expression were calculated using negative binomial generalized linear model (NB-GLM). Different letters above boxplots indicate significant differences (polygalacturonase: $n = 9$, $X^2 = 14.7$, $df = 2$, $p < 0.001$; α -glucuronidase: $n = 9$, $X^2 = 25$, $df = 2$, $p < 0.005$).

(E) Symbiont plasmid copy number per chromosome across host compartments. This was determined by dividing the polygalacturonase copy number by the copy number of the chromosomal genes: 16S rRNA (left) and the chaperonin *groL* (right). Differences in plasmid copy number were estimated using a general linear model (LM) (16S rRNA: $n = 9$, $F_{(2,4)} = 26.3$, $df = 2$, $p = 0.0049$, *groL*: $n = 9$, $F_{(2,4)} = 10.37$, $df = 2$, $p = 0.0261$). Different letters above boxplots indicate significant differences ($p < 0.05$).

See also Data S4 and S5.

that reflects its beneficial role.⁸ Specifically, the gene encoding for polygalacturonase is the 4th most highly expressed transcript, behind ribosomal proteins, but ahead of chaperones such as *groL*, *groS*, and *dnaK*.⁸ These patterns are in line with

the transcriptomes of obligate endosymbionts in other insect groups, where genes coding for chaperones and host-beneficial factors (e.g., essential amino acids) are among the most highly expressed.⁴⁶ But given the symbiont's extracellular localization within its host and during transmission,⁸ we aimed to quantify the symbiont's transcriptional plasticity relative to host development and nutritional requirements. To address this, we compared the transcriptional profiles of *Stammera* within the foregut symbiotic organs of larvae and adults, as well as egg caplets in the tortoise beetle, *C. alternans* (Figure 5A).

Like other cassidines, *C. alternans* relies on egg caplets to vertically transmit *Stammera*.^{3,6,7} *Stammera* is embedded within spherical secretions during transmission and remains separated from the developing embryo until larval eclosion⁷ (Figure 5A). This contrasts symbiont localization within foregut symbiotic organs in larvae and adults (Figure 5A), where *Stammera* is already

acquired and is contributing to *C. alternans* digestion and development.^{4,7} Reflecting these differences, we quantified a dynamic transcriptional profile across treatments (Figures 5B and 5C; permuted multivariate analysis of variance [PERMANOVA], $p = 0.003$). By comparing the transcriptional activity of *Stammera* within egg caplets relative to larval and adult foregut symbiotic organs (Figures 5B and 5C), we observe 59 and 65 genes to be differentially expressed, respectively (Data S4A and S4B; false discovery rate [FDR]-adjusted $p < 0.05$). Most of these genes are shared (52 in total), highlighting a functional overlap in the transcriptional differences affecting *Stammera* during transmission relative to its localization within foregut symbiotic organs (Figure 5C; Data S4A and S4B). By contrast, only 19 *Stammera* genes are differentially expressed between larvae and adult beetles (Data S4C; FDR-adjusted $p < 0.05$), indicative of a consistent transcriptional profile within symbiotic organs that are morphologically conserved throughout development (Figures 5A–5C).⁹

Genes that are preferentially expressed in egg caplets relative to the foregut symbiotic organs largely encode chaperones and tolerance proteins (e.g., *cspE*) (Data S4D and S4E; FDR-adjusted $p < 0.05$). These dynamics may reflect the abiotic challenges *Stammera* contends with during extracellular transfer.¹⁰ On average, *Stammera* must subsist for 11 days within the egg caplet prior to acquisition by its host.^{7,9} Hence, the symbiont may be modulating its metabolism to buffer fluctuations in temperature and humidity,^{7,47} as experienced by other extracellularly transmitted insect symbionts such as *Ishikawaella*,¹² *Burkholderia*,^{11,48} and *Pantoea*.¹⁴

By contrast, symbiont genes involved in carbohydrate transport and metabolism are upregulated within the foregut symbiotic organs of both larvae and adults relative to the egg caplet (Data S4F and S4G; FDR-adjusted $p < 0.05$), including the two digestive enzymes supplemented by *Stammera* to *C. alternans* (Figure 5D): polygalacturonase (negative binomial generalized linear model [GLM] $X^2 = 14.7$, $df = 2$, $p < 0.001$, average \log_2 foldchange = 1.27) and α -glucuronidase (negative binomial GLM $X^2 = 25$, $df = 2$, $p < 0.001$, average \log_2 foldchange = 1.77). The elevated expression of both genes aligns with the nutritional requirements of larvae and adults since both stages are actively engaged in folivory,^{47,49} in contrast to eggs.

Most endosymbionts possessing drastically reduced genomes (<0.25 Mb) maintain a rudimentary transcriptional machinery,⁴¹ limiting their potential to regulate gene expression.⁴⁶ Of the transcription-related genes consistently retained within such tiny genomes, including *Stammera*'s, only *rpoA*, *rpoB*, *rpoC*, and *rpoD* are conserved.⁴¹ But in contrast to intracellular symbionts such as *Carsonella* (0.16 Mb) in psyllids,⁵⁰ *Hodgkinia* (0.14 Mb) in cicadas,^{36,51} and *Nasuia* (0.11 Mb) in leafhoppers,³¹ the extracellular *Stammera* additionally retained a broader collection of transcriptional regulators, featuring *rpoH*, *rpoZ*, *nusA*, *nusB*, *nusG*, and *rho* (Data S5). As major regulators of bacterial transcription elongation, the annotation of *nusA* and *nusG* is especially notable, since both factors modulate intrinsic and Rho-dependent termination by binding to RNA polymerase.^{52,53} A greater transcriptional control may reflect the extracellular localization of *Stammera* (Figure 5A) and the instability of life beyond the metabolic comforts of a host cell.

Since polygalacturonase and α -glucuronidase are both plasmid-encoded, we also examined whether *Stammera* can elevate their expression by increasing plasmid abundance. We observe that plasmid copy numbers do increase following larval eclosion from the egg and through adulthood (Figure 5E; linear model [LM], *16S rRNA* [$F_{(2,4)} = 26.3$, $p = 0.0049$] and *groL* [$F_{(2,4)} = 10.3$, $p = 0.026$]). Modulating plasmid abundance to meet host nutritional requirements is shown in other insect-microbe symbioses, including *Buchnera* in aphids.⁵⁴ *Buchnera* genes responsible for the biosynthesis of leucine, an essential amino acid, are encoded on the pLeu plasmid.⁵⁵ In response to leucine starvation in the host, *Buchnera* increases pLeu plasmid copy numbers, mirroring the dynamics observed in *Stammera* relative to beetle development and nutritional requirements (Figure 5E).

Early diverging, non-symbiotic cassidines encode polygalacturonase endogenously

As the sole plant cell wall-degrading enzyme universally encoded by *Stammera*, polygalacturonase is critical for origin and stability of symbiosis within the Cassidinae (Figure 4). The pectinase similarly underpins the partnership between *Macropheicola* and reed beetles (Chrysomelidae: Donaciinae),⁵⁶ highlighting a functional convergence of digestive symbioses in folivorous insects.⁵⁷ Given the foundational role of polygalacturonase for leaf beetle-bacterial symbioses⁵⁸ and the obligate dependence of cassidines on *Stammera*,^{3,7} we aimed to clarify how non-symbiotic members of the subfamily contend with a leafy diet enriched in pectin.

In addition to symbiosis, horizontal gene transfer from bacteria and fungi endowed herbivorous beetles with catalytic tools to deconstruct complex plant polymers.^{2,59} The two independent origins of herbivory in beetles coincided with the cooption of microbial plant cell wall-degrading enzymes,² including polygalacturonase.⁵⁹ Although symbiotic cassidines maintain cellulases endogenously, beetle-encoded polygalacturonases were lost,⁴ suggesting that the acquisition of *Stammera* may have relaxed selection to retain the enzyme. To explore whether early diverging, non-symbiotic members of the subfamily encode the pectinase endogenously, we characterized the plant cell wall-degrading enzymes maintained by *Calyptocephala attenuata*, a hispine beetle belonging to the Spilophorini tribe (Figure 1B). By combining long-read high fidelity (HiFi) genome sequencing from Pacific Biosciences with RNA sequencing on an Illumina NextSeq 2000 system, we observe that *C. attenuata* encodes the same set of cellulases (GH9, 45, and 48) and xylanases (GH10) as symbiotic members of the Cassidinae (Figure 6). But by contrast, we also annotated polygalacturonase-encoding genes on three separate beetle contigs (Figure 6A), ranging in size between 25 and 45 kb and flanked by insect genes. Intron content and TATA-box localization further clarified the eukaryotic features of these genes, coupled with our ability to amplify them by PCR using DNA extractions from the legs, thorax, and elytra of *C. attenuata*. All three copies of the gene retained the key catalytic residues described for polygalacturonase (Figure 6A),^{60,61} indicating that the encoded enzymes are functionally conserved and likely confer a pectinolytic phenotype in the absence of *Stammera*. Pectinases encoded by *C. attenuata* align most closely with non-*Stammera*, bacterial polygalacturonases

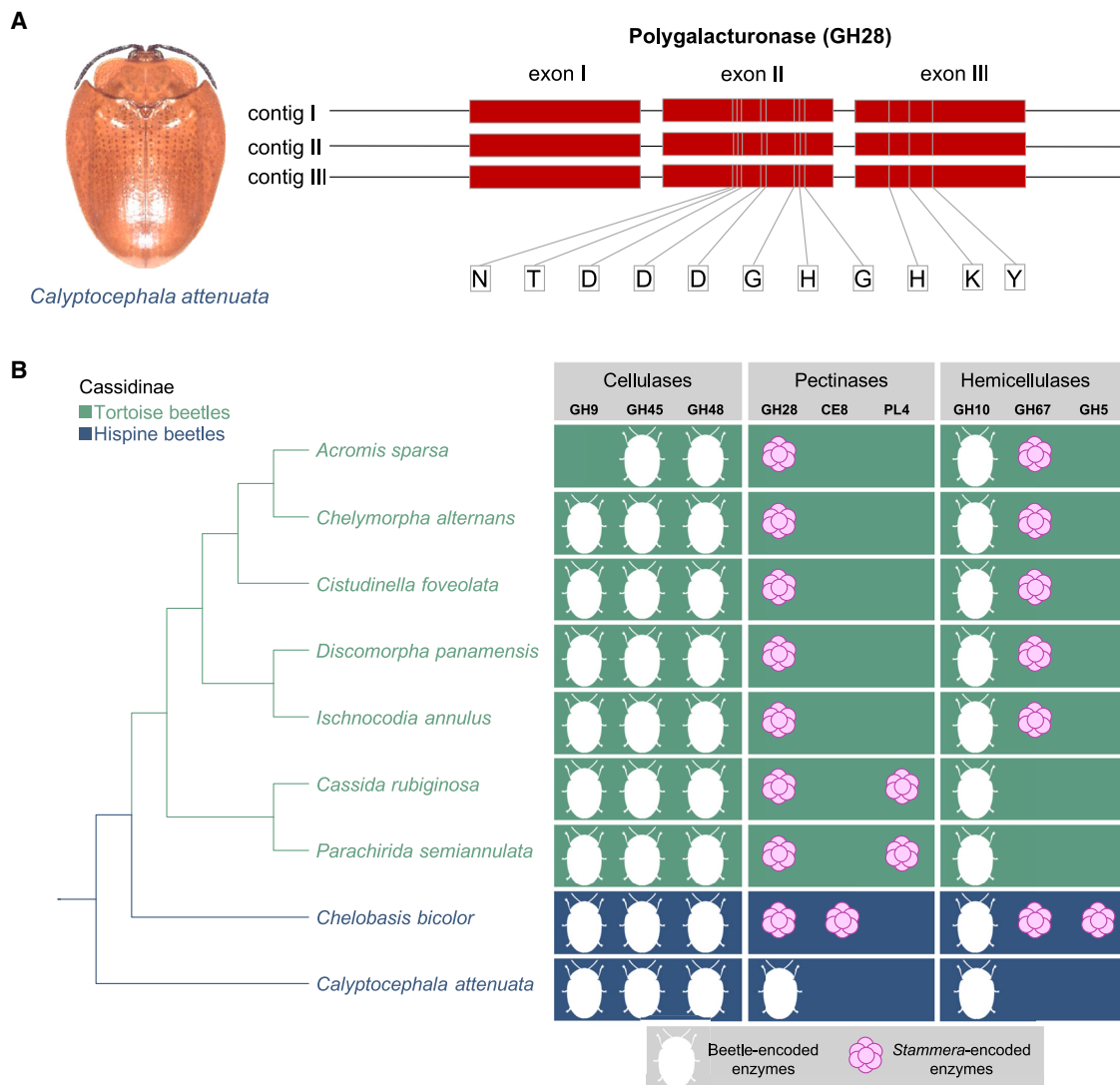


Figure 6. Early diverging, non-symbiotic cassidines encode polygalacturonase endogenously

(A) The early diverging, non-symbiotic hispine beetle *Calyptocephala attenuata*. Gene structure and functionally conserved amino acids across the three copies of the polygalacturonase-encoding gene from *C. attenuata* draft genome assembly.

(B) Distribution of host- and *Stammera*-encoded plant cell wall-degrading enzymes as inferred from transcriptome and symbiont genome profiling of nine representative cassidine species (tortoise beetles in green, hispines in blue). Source of each digestive enzyme is designated by an icon. Abbreviations are as follows: GH, glycoside hydrolase; CE, carbohydrate esterase; and PL, polysaccharide lyase.

See also [Figures S4](#) and [S5](#) and [Table S1](#).

([Figure S5](#)), similar to bruchine beetles,⁶² but in contrast to the ancestral configuration of endogenous polygalacturonases across the Chrysomelidae, which are of fungal origin.⁵⁹

Given the adaptive importance of polygalacturonase for herbivorous beetles,^{59,63} it is unclear how pectinolysis was outsourced to *Stammera* in symbiotic cassidines ([Figure 6B](#)).^{3,4} It is conceivable that deleterious mutations may have compromised the functionality of beetle-encoded pectinases, necessitating rescue through symbiosis with a beneficial microbe. Several herbivorous beetles retain a repertoire of functionally active and inactive polygalacturonases,^{59,64} where the latter can no longer bind homogalacturonan due to amino acid substitutions at crucial positions.⁶⁵ It is also possible that the presence

of a symbiotic copy of polygalacturonase may have permitted the neutral loss of the host-encoded enzyme, irrespective of whether selection favored one at the expense of the other. Finally, symbiont acquisition may have spurred evolutionary innovation by upgrading the digestive abilities of a subset of cassidines, rendering endogenous polygalacturonases redundant. All three scenarios are not mutually exclusive and may have occurred in a stepwise process. Although non-symbiotic cassidines retained polygalacturonase endogenously ([Figure 6B](#)), the ancestral configuration of enzymes derived from *Stammera* included polygalacturonase in addition to rhamnogalacturonan lyase and α -glucuronidase ([Figure 4A](#)). While speculative, by expanding the range of universal plant polymers that an herbivore

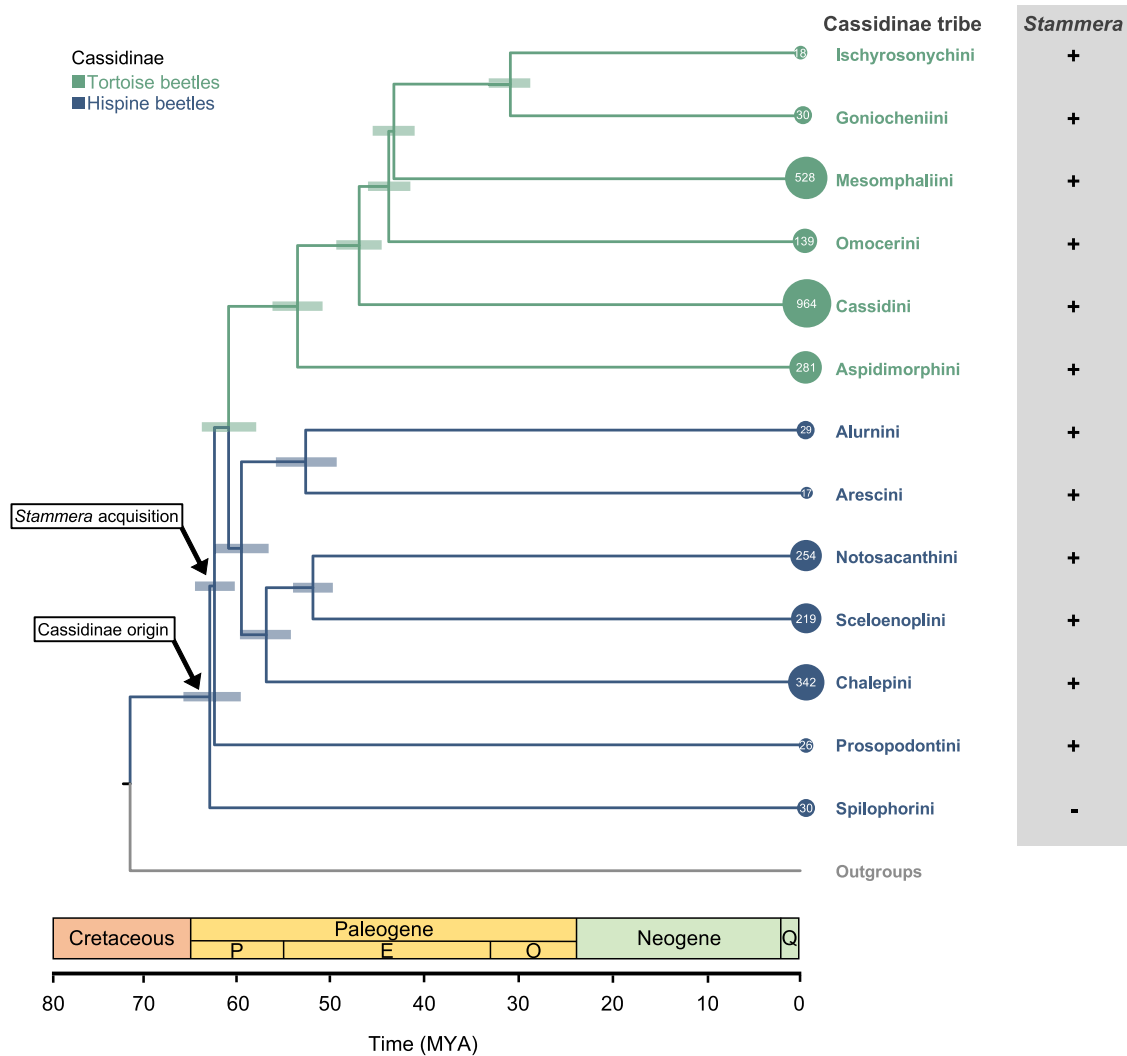


Figure 7. Symbiont acquisition relative to the evolutionary history of Cassidinae beetles

Time-calibrated phylogeny dating the origin of the Cassidinae subfamily and the timing of *Stammera* acquisition. Branches are colored to differentiate hispine (blue) from tortoise beetle tribes (green). Circle sizes (and their enclosed numbers) correspond to the species richness of each Cassidinae tribe. Bars depict confidence intervals (95% highest posterior density) of node ages. Symbols (±) denote the symbiotic status of each tribe. Abbreviations are as follows: P, Paleocene; E, Eocene; O, Oligocene; and Q, Quaternary. See also [Figures S6](#) and [S7](#) and [Table S2](#).

can deconstruct ([Figures 4](#) and [6](#)), *Stammera* may have relaxed the need for its host to maintain polygalacturonase and/or compensated for their reduced efficiency.

Beetle diversification following symbiont acquisition

Symbioses are key drivers of global biodiversity.^{66,67} By facilitating access to new environments or by allowing organisms to integrate novel metabolic features, mutualistic partnerships can promote diversification by increasing speciation rates and/or decreasing the rate of extinction.^{66,67} The consequences of beneficial partnerships on species richness are most evident when net diversification rates are compared between symbiotic and non-symbiotic members of a clade. In gall-inducing midges, for example, the acquisition of a fungal nutritional symbiont resulted in a seven-fold expansion in the range of suitable host-

plant taxa relative to lineages that do not stably associate with a fungus.⁶⁸ Correspondingly, net diversification of symbiotic midges outpaced that of their non-symbiotic relatives by 17 times.⁶⁸

Among cassidines, the loss of endogenous polygalacturonases coincided with the acquisition of a symbiont supplementing a broader collection of pectinases and other digestive enzymes ([Figure 6B](#)). Given the expanded metabolic potential of symbiotic cassidines relative to non-symbiotic taxa, we quantified how *Stammera* acquisition may have impacted the diversification rate, species richness, and plant use by its host. Three fossil calibration points were used to infer the minimum ages of divergence within the Cassidinae phylogeny, including *Notosacanthini*, *Chalepini*, and *Cassidini* specimens dated at 47,⁶⁹ 44.1,¹⁸ and 40 mya,⁷⁰ respectively. The resulting time-calibrated

phylogeny revealed that the symbiosis formed 62 mya (95% confidence interval [CI]: 59.9–64.3), soon after the Paleocene origin of the Cassidinae subfamily (62.5 mya; 95% CI: 59.36–65.59) (Figures 7 and S6; Table S2). By applying estimates of tribe-level species richness within the Cassidinae,¹⁷ net diversification rates were quantified relative to the symbiotic condition using Modeling Evolutionary Diversification Using Stepwise Akaike Information Criterion (MEDUSA) and as implemented in the Geiger package.⁷¹ Our analysis revealed a background speciation rate of 0.0557 (lineages/Ma) and located two diversification shifts (Figure S7). A net increase rate followed *Stammera* acquisition (Figure S7; 0.1237 lineages/Ma), potentially implicating symbiosis in the ecological radiation of the Cassidinae subfamily and its accumulation of species diversity (Figure 7). This is concordant with our comparison of species richness and host-plant use of symbiotic and non-symbiotic cassidines. We observe that *Stammera*-harboring tribes are significantly more speciose (Figure 7) (G test, $n = 2,877$, $G = 182.14$, $df = 1$, $p < 0.001$) and exploit a greater variety of plant families (G test, $n = 48$, $G = 43.64$, $df = 1$, $p < 0.001$). A second, and more derived, diversification rate shift featured a slowdown in two symbiotic hispine clades, the Alurnini and Arescini (Figure S7; 0.0594 lineages/Ma). These feature specialists on the immature rolled leaves of plants in the monocotyledonous genus *Heliconia*.¹⁹ McKenna and Farrell¹⁸ report similar decelerations in *Heliconia*-feeding hispine beetles, suggesting that niche specialization may decrease origination rates among cassidines irrespective of an association with *Stammera*.

Conclusions

Symbioses evolved across several highly diverse insect clades in conjunction with key traits to facilitate herbivory.^{32,58,72–75} Through the supplementation of nutrients to balance a specialized diet,^{31,75,76} or the production of enzymes to overcome complex plant molecules and toxins,^{73,77–79} symbiont acquisition and evolution are key determinants of host-plant use.⁸⁰ Despite marked differences in their nutritional ecology, here we report on a shared symbiosis between tortoise and hispine beetles, offering insights into the origin and ancestral configuration of a Paleocene-age partnership with *Stammera*. In light of an up-graded metabolic potential following symbiont acquisition, *Stammera*-harboring cassidines are more speciose and exploit a greater variety of plants, highlighting the adaptive impact of a symbiotic transition.

STAR★METHODS

Detailed methods are provided in the online version of this paper and include the following:

- KEY RESOURCES TABLE
- RESOURCE AVAILABILITY
 - Lead contact
 - Materials availability
 - Data and code availability
- EXPERIMENTAL MODEL AND STUDY PARTICIPANT DETAILS
- METHOD DETAILS
 - Genome sequencing and assembly

- *Stammera* comparative genomics
- Symbiont phylogenetic reconstruction
- *Stammera* molecular evolution
- Ancestral state reconstruction
- Host phylogenetic reconstruction
- Host-symbiont cophylogenetic analysis
- Diversification rate analyses
- Symbiont transcriptome sequencing
- Quantitative PCR
- Long-read sequencing and beetle genome assembly
- Host RNAseq, transcriptome assembly, and CAZY annotation
- Thin layer chromatography (TLC)
- Fluorescence *in situ* hybridization (FISH)
- QUANTIFICATION AND STATISTICAL ANALYSIS

SUPPLEMENTAL INFORMATION

Supplemental information can be found online at <https://doi.org/10.1016/j.cub.2024.01.070>.

ACKNOWLEDGMENTS

Financial support from the Max Planck Society, German Research Foundation (SA 3105/2-1, BE 6922/1-1, and EXC2124—390838134), Japan Science and Technology Agency (JST) (ERATO grant JPMJER1902), European Molecular Biology Organization, and Alexander Von Humboldt Foundation is gratefully acknowledged. This study complies with Nagoya Protocol regulations in the Republic of Panama and France per the following permits: ARG-027-2023 and TREL2302365S/693. We thank Julie Johnson (Life Sciences Studios) for the illustrations in Figure 1D and Lech Borowiec for the *Calyptocephala attenuata* image.

AUTHOR CONTRIBUTIONS

M.G.-L. and H.S. conceived of the study. M.G.-L., D.W., and H.S. designed experiments. M.G.-L., C.H., D.W., I.P., A.B., C.L., H.B., K.O., Y.M., S.G., Y.P., T.F., M.A.G.P., and H.S. carried out experiments, sequencing work, and analysis. M.G.-L. and H.S. wrote the manuscript. All authors edited and commented on the paper.

DECLARATION OF INTERESTS

The authors declare no competing interests.

Received: December 18, 2023

Revised: January 22, 2024

Accepted: January 29, 2024

Published: February 19, 2024

REFERENCES

1. Karasov, W.H., and del Rio, C.M. (2020). *Physiological Ecology: How Animals Process Energy, Nutrients, and Toxins* (Princeton University Press).
2. McKenna, D.D., Shin, S., Ahrens, D., Balke, M., Beza-Beza, C., Clarke, D.J., Donath, A., Escalona, H.E., Friedrich, F., Letsch, H., et al. (2019). The evolution and genomic basis of beetle diversity. *Proc. Natl. Acad. Sci. USA* **116**, 24729–24737.
3. Salem, H., Bauer, E., Kirsch, R., Berasategui, A., Cripps, M., Weiss, B., Koga, R., Fukumori, K., Vogel, H., Fukatsu, T., et al. (2017). Drastic genome reduction in an herbivore's pectinolytic symbiont. *Cell* **171**, 1520–1531.e13.
4. Salem, H., Kirsch, R., Pauchet, Y., Berasategui, A., Fukumori, K., Moriyama, M., Cripps, M., Windsor, D., Fukatsu, T., and Gerardo, N.M.

- (2020). Symbiont digestive range reflects host plant breadth in herbivorous beetles. *Curr. Biol.* **30**, 2875–2886.e4.
5. Stammer, H.-J. (1936). Studien an Symbiosen zwischen Käfern und Mikroorganismen. *Zeitschrift für Morphologie und Ökologie der Tiere* **31**, 682–697.
 6. Fukumori, K., Oguchi, K., Ikeda, H., Shinohara, T., Tanahashi, M., Moriyama, M., Koga, R., and Fukatsu, T. (2022). Evolutionary dynamics of host organs for microbial symbiosis in tortoise leaf beetles (Coleoptera: Chrysomelidae: Cassidinae). *mBio* **13**, e0369121.
 7. Pons, I., González Porras, M.Á., Breitenbach, N., Berger, J., Hipp, K., and Salem, H. (2022). For the road: calibrated maternal investment in light of extracellular symbiont transmission. *Proc. Biol. Sci.* **289**, 20220386.
 8. Bauer, E., Kaltenpoth, M., and Salem, H. (2020). Minimal fermentative metabolism fuels extracellular symbiont in a leaf beetle. *ISME J.* **14**, 866–870.
 9. Porras, M.Á.G., Pons, I., García-Lozano, M., Jagdale, S., Emmerich, C., Weiss, B., and Salem, H. (2024). Extracellular symbiont colonizes insect during embryo development. *ISME Commun.* **4**, ycae005.
 10. Salem, H., Florez, L., Gerardo, N., and Kaltenpoth, M. (2015). An out-of-body experience: the extracellular dimension for the transmission of mutualistic bacteria in insects. *Proc. Biol. Sci.* **282**, 20142957.
 11. Kikuchi, Y., Hosokawa, T., and Fukatsu, T. (2007). Insect-microbe mutualism without vertical transmission: a stinkbug acquires a beneficial gut symbiont from the environment every generation. *Appl. Environ. Microbiol.* **73**, 4308–4316.
 12. Koga, R., Tanahashi, M., Nikoh, N., Hosokawa, T., Meng, X.Y., Moriyama, M., and Fukatsu, T. (2021). Host's guardian protein counters degenerative symbiont evolution. *Proc. Natl. Acad. Sci. USA* **118**, e2103957118.
 13. Salem, H., Onchuru, T.O., Bauer, E., and Kaltenpoth, M. (2015). Symbiont transmission entails the risk of parasite infection. *Biol. Lett.* **11**, 20150840.
 14. Hosokawa, T., Ishii, Y., Nikoh, N., Fujie, M., Satoh, N., and Fukatsu, T. (2016). Obligate bacterial mutualists evolving from environmental bacteria in natural insect populations. *Nat. Microbiol.* **1**, 15011.
 15. Koch, H., and Schmid-Hempel, P. (2011). Socially transmitted gut microbiota protect bumble bees against an intestinal parasite. *Proc. Natl. Acad. Sci. USA* **108**, 19288–19292.
 16. Marsh, S.E., Poulsen, M., Pinto-Tomás, A., and Currie, C.R. (2014). Interaction between workers during a short time window is required for bacterial symbiont transmission in *Acromyrmex* leaf-cutting ants. *PLoS One* **9**, e103269.
 17. Chaboo, C.S. (2007). Biology and phylogeny of the Cassidinae Gyllenhal sensu lato (tortoise and leaf-mining beetles) (Coleoptera: Chrysomelidae). *Bull. Am. Mus. Nat. Hist.* **305**, 1–250.
 18. McKenna, D.D., and Farrell, B.D. (2006). Tropical forests are both evolutionary cradles and museums of leaf beetle diversity. *Proc. Natl. Acad. Sci. USA* **103**, 10947–10951.
 19. McKenna, D.D., and Farrell, B.D. (2005). Molecular phylogenetics and evolution of host plant use in the Neotropical rolled leaf “hispine” beetle genus *Cephaloleia* (Chevrolat) (Chrysomelidae: Cassidinae). *Mol. Phylogenet. Evol.* **37**, 117–131.
 20. Barrows, E.M. (1979). Life cycles, mating, and color change in tortoise beetles (Coleoptera: Chrysomelidae: Cassidinae). *Coleopt. Bull.* **33**, 9–16.
 21. Zeng, L., Zhang, N., Zhang, Q., Endress, P.K., Huang, J., and Ma, H. (2017). Resolution of deep eudicot phylogeny and their temporal diversification using nuclear genes from transcriptomic and genomic datasets. *New Phytol.* **214**, 1338–1354.
 22. Barraclough, T.G., Barclay, M.V., and Vogler, A.P. (1998). Species richness: does flower power explain beetle-mania? *Curr. Biol.* **8**, R843–R845.
 23. Blankenchip, C.L., Michels, D.E., Braker, H.E., and Goffredi, S.K. (2018). Diet breadth and exploitation of exotic plants shift the core microbiome of *Cephaloleia*, a group of tropical herbivorous beetles. *PeerJ* **6**, e4793.
 24. Chong, R.A., Park, H., and Moran, N.A. (2019). Genome evolution of the obligate endosymbiont *Buchnera aphidicola*. *Mol. Biol. Evol.* **36**, 1481–1489.
 25. Wang, D., Huang, Z., Billen, J., Zhang, G., He, H., and Wei, C. (2021). Structural diversity of symbionts and related cellular mechanisms underlying vertical symbiont transmission in cicadas. *Environ. Microbiol.* **23**, 6603–6621.
 26. Hosokawa, T., Kikuchi, Y., Nikoh, N., Shimada, M., and Fukatsu, T. (2006). Strict host-symbiont cospeciation and reductive genome evolution in insect gut bacteria. *PLoS Biol.* **4**, e337.
 27. Hosokawa, T., Nikoh, N., Koga, R., Satô, M., Tanahashi, M., Meng, X.Y., and Fukatsu, T. (2012). Reductive genome evolution, host-symbiont cospeciation and uterine transmission of endosymbiotic bacteria in bat flies. *ISME J.* **6**, 577–587.
 28. Konstantinidis, K.T., and Tiedje, J.M. (2004). Trends between gene content and genome size in prokaryotic species with larger genomes. *Proc. Natl. Acad. Sci. USA* **101**, 3160–3165.
 29. Bennett, G.M., McCutcheon, J.P., McDonald, B.R., and Moran, N.A. (2015). Lineage-specific patterns of genome deterioration in obligate symbionts of sharpshooter leafhoppers. *Genome Biol. Evol.* **8**, 296–301.
 30. Eren, A.M., Kiehl, E., Shaiber, A., Veseli, I., Miller, S.E., Schechter, M.S., Fink, I., Pan, J.N., Yousef, M., Fogarty, E.C., et al. (2021). Community-led, integrated, reproducible multi-omics with anvio. *Nat. Microbiol.* **6**, 3–6.
 31. Bennett, G.M., and Moran, N.A. (2013). Small, smaller, smallest: the origins and evolution of ancient dual symbioses in a phloem-feeding insect. *Genome Biol. Evol.* **5**, 1675–1688.
 32. Bennett, G.M., and Moran, N.A. (2015). Heritable symbiosis: The advantages and perils of an evolutionary rabbit hole. *Proc. Natl. Acad. Sci. USA* **112**, 10169–10176.
 33. Vasquez, Y.M., and Bennett, G.M. (2022). A complex interplay of evolutionary forces continues to shape ancient co-occurring symbiont genomes. *iScience* **25**, 104786.
 34. Perreau, J., and Moran, N.A. (2022). Genetic innovations in animal-microbe symbioses. *Nat. Rev. Genet.* **23**, 23–39.
 35. Poliakov, A., Russell, C.W., Ponnala, L., Hoops, H.J., Sun, Q., Douglas, A.E., and van Wijk, K.J. (2011). Large-scale label-free quantitative proteomics of the pea aphid-*Buchnera* symbiosis. *Mol. Cell. Proteomics* **10**, M110.007039.
 36. Van Leuven, J.T., and McCutcheon, J.P. (2012). An AT mutational bias in the tiny GC-rich endosymbiont genome of *Hodgkinia*. *Genome Biol. Evol.* **4**, 24–27.
 37. Kjeldsen, K.U., Bataillon, T., Pinel, N., De Mita, S., Lund, M.B., Panitz, F., Bendixen, C., Stahl, D.A., and Schramm, A. (2012). Purifying selection and molecular adaptation in the genome of *Verminephrobacter*, the heritable symbiotic bacteria of earthworms. *Genome Biol. Evol.* **4**, 307–315.
 38. Yang, Z. (2007). PAML 4: phylogenetic analysis by maximum likelihood. *Mol. Biol. Evol.* **24**, 1586–1591.
 39. Sabater-Muñoz, B., Toft, C., Alvarez-Ponce, D., and Fares, M.A. (2017). Chance and necessity in the genome evolution of endosymbiotic bacteria of insects. *ISME J.* **11**, 1291–1304.
 40. Osvatic, J.T., Yuen, B., Kunert, M., Wilkins, L., Hausmann, B., Girguis, P., Lundin, K., Taylor, J., Jospin, G., and Petersen, J.M. (2023). Gene loss and symbiont switching during adaptation to the deep sea in a globally distributed symbiosis. *ISME J.* **17**, 453–466.
 41. McCutcheon, J.P., and Moran, N.A. (2011). Extreme genome reduction in symbiotic bacteria. *Nat. Rev. Microbiol.* **10**, 13–26.
 42. Maddison, W., and Maddison, D. (2023). Mesquite: a modular system for evolutionary analysis. <http://www.mesquiteproject.org>.
 43. Harris, P.J. (2005). Diversity in plant cell walls. In *Plant Diversity and Evolution: Genotypic and Phenotypic Variation in Higher Plants* (CABI Publishing), pp. 201–227.
 44. Davé, V., and McCarthy, S.P. (1997). Review of konjac glucomannan. *J. Environ. Polym. Degrad.* **5**, 237–241.

45. Tailford, L.E., Ducros, V.M.-A., Flint, J.E., Roberts, S.M., Morland, C., Zechel, D.L., Smith, N., Bjørnvad, M.E., Borchert, T.V., Wilson, K.S., et al. (2009). Understanding how diverse beta-mannanases recognize heterogeneous substrates. *Biochemistry* *48*, 7009–7018.
46. Bennett, G.M., and Chong, R.A. (2017). Genome-wide transcriptional dynamics in the companion bacterial symbionts of the glassy-winged sharpshooter (Cicadellidae: *Homalodisca vitripennis*) reveal differential gene expression in bacteria occupying multiple host organs. *G3 (Bethesda)* *7*, 3073–3082.
47. Morrison, C.R., and Windsor, D.M. (2018). The life history of *Chelymormpha alternans* (Coleoptera: Chrysomelidae: Cassidinae) in Panamá. *Ann. Entomol. Soc. Am.* *111*, 31–41.
48. Ohbayashi, T., Futahashi, R., Terashima, M., Barrière, Q., Lamouche, F., Takeshita, K., Meng, X.Y., Mitani, Y., Sone, T., Shigenobu, S., et al. (2019). Comparative cytology, physiology and transcriptomics of Burkholderia insecticola in symbiosis with the bean bug Riptortus pedestris and in culture. *ISME J.* *13*, 1469–1483.
49. Morrison, C.R., Aubert, C., and Windsor, D.M. (2019). Variation in host plant usage and diet breadth predict sibling preference and performance in the neotropical tortoise beetle *Chelymormpha alternans* (Coleoptera: Chrysomelidae: Cassidinae). *Environ. Entomol.* *48*, 382–394.
50. Nakabachi, A., Yamashita, A., Toh, H., Ishikawa, H., Dunbar, H.E., Moran, N.A., and Hattori, M. (2006). The 160-kilobase genome of the bacterial endosymbiont *Carsonella*. *Science* *314*, 267.
51. Campbell, M.A., Van Leuven, J.T., Meister, R.C., Carey, K.M., Simon, C., and McCutcheon, J.P. (2015). Genome expansion via lineage splitting and genome reduction in the cicada endosymbiont *Hodgkinia*. *Proc. Natl. Acad. Sci. USA* *112*, 10192–10199.
52. Strauß, M., Vitiello, C., Schweimer, K., Gottesman, M., Rösch, P., and Knauer, S.H. (2016). Transcription is regulated by NusA:NusG interaction. *Nucleic Acids Res.* *44*, 5971–5982.
53. Mandell, Z.F., Oshiro, R.T., Yakhnin, A.V., Vishwakarma, R., Kashlev, M., Kearns, D.B., and Babitzke, P. (2021). NusG is an intrinsic transcription termination factor that stimulates motility and coordinates gene expression with NusA. *eLife* *10*, e61880.
54. Viñuelas, J., Febvay, G., Duport, G., Colella, S., Fayard, J.M., Charles, H., Rahbé, Y., and Calevro, F. (2011). Multimodal dynamic response of the *Buchnera aphidicola* pLeu plasmid to variations in leucine demand of its host, the pea aphid *Acyrtosiphon pisum*. *Mol. Microbiol.* *81*, 1271–1285.
55. Latorre, A., Gil, R., Silva, F.J., and Moya, A. (2005). Chromosomal stasis versus plasmid plasticity in aphid endosymbiont *Buchnera aphidicola*. *Heredity* *95*, 339–347.
56. Reis, F., Kirsch, R., Pauchet, Y., Bauer, E., Bilz, L.C., Fukumori, K., Fukatsu, T., Kölsch, G., and Kaltenpoth, M. (2020). Bacterial symbionts support larval sap feeding and adult folivory in (semi-)aquatic reed beetles. *Nat. Commun.* *11*, 2964.
57. Berasategui, A., and Salem, H. (2020). Microbial determinants of folivory in insects. In *Cellular Dialogues in the Holobiont*, T.C.G. Bosch, and M.G. Hadfield, eds. (CRC Press), pp. 217–232.
58. Salem, H., and Kaltenpoth, M. (2022). Beetle–bacterial symbioses: Endless forms most functional. *Annu. Rev. Entomol.* *67*, 201–219.
59. Kirsch, R., Gramzow, L., Theißen, G., Siegfried, B.D., Ffrench-Constant, R.H., Heckel, D.G., and Pauchet, Y. (2014). Horizontal gene transfer and functional diversification of plant cell wall degrading polygalacturonases: Key events in the evolution of herbivory in beetles. *Insect Biochem. Mol. Biol.* *52*, 33–50.
60. Armand, S., Wagemaker, M.J.M., Sánchez-Torres, P., Kester, H.C.M., van Santen, Y., Dijkstra, B.W., Visser, J., and Benen, J.A.E. (2000). The active site topology of *Aspergillus niger* endopolygalacturonase II as studied by site-directed mutagenesis. *J. Biol. Chem.* *275*, 691–696.
61. Kester, H.C., Kusters-van Someren, M.A., Müller, Y., and Visser, J. (1996). Primary structure and characterization of an exopolygalacturonase from *Aspergillus tubingensis*. *Eur. J. Biochem.* *240*, 738–746.
62. Busch, A., Kunert, G., Heckel, D.G., and Pauchet, Y. (2017). Evolution and functional characterization of CAZymes belonging to subfamily 10 of glycoside hydrolase family 5 (GH5_10) in two species of phytophagous beetles. *PLoS One* *12*, e0184305.
63. Kirsch, R., Okamura, Y., Haeger, W., Vogel, H., Kunert, G., and Pauchet, Y. (2022). Metabolic novelty originating from horizontal gene transfer is essential for leaf beetle survival. *Proc. Natl. Acad. Sci. USA* *119*, e2205857119.
64. Kirsch, R., Heckel, D.G., and Pauchet, Y. (2016). How the rice weevil breaks down the pectin network: Enzymatic synergism and sub-functionalization. *Insect Biochem. Mol. Biol.* *71*, 72–82.
65. Kirsch, R., Kunert, G., Vogel, H., and Pauchet, Y. (2019). Pectin digestion in herbivorous beetles: Impact of pseudoenzymes exceeds that of their active counterparts. *Front. Physiol.* *10*, 685.
66. Chomicki, G., Weber, M., Antonelli, A., Bascompte, J., and Kiers, E.T. (2019). The impact of mutualisms on species richness. *Trends Ecol. Evol.* *34*, 698–711.
67. Cornwallis, C.K., van 't Padje, A., Ellers, J., Klein, M., Jackson, R., Kiers, E.T., West, S.A., and Henry, L.M. (2023). Symbioses shape feeding niches and diversification across insects. *Nat. Ecol. Evol.* *7*, 1022–1044.
68. Joy, J.B. (2013). Symbiosis catalyses niche expansion and diversification. *Proc. Biol. Sci.* *280*, 20122820.
69. Chaboo, C.S., and Engel, M.S. (2009). Eocene tortoise beetles from the Green River Formation in Colorado, U.S.A. (Coleoptera: Chrysomelidae: Cassidinae). *Syst. Entomol.* *34*, 202–209.
70. Poinar, G.O. (1999). Chrysomelidae in fossilized resin: behavioural inferences. In *Advances in Chrysomelidae Biology*, M.L. Cox, ed., pp. 1–16.
71. Alfaro, M.E., Santini, F., Brock, C., Alamillo, H., Dornburg, A., Rabosky, D.L., Carnevale, G., and Harmon, L.J. (2009). Nine exceptional radiations plus high turnover explain species diversity in jawed vertebrates. *Proc. Natl. Acad. Sci. USA* *106*, 13410–13414.
72. Hansen, A.K., and Moran, N.A. (2014). The impact of microbial symbionts on host plant utilization by herbivorous insects. *Mol. Ecol.* *23*, 1473–1496.
73. Brune, A. (2014). Symbiotic digestion of lignocellulose in termite guts. *Nat. Rev. Microbiol.* *12*, 168–180.
74. Kwong, W.K., and Moran, N.A. (2016). Gut microbial communities of social bees. *Nat. Rev. Microbiol.* *14*, 374–384.
75. Jackson, R., Monnin, D., Patapiou, P.A., Golding, G., Helanterä, H., Oettler, J., Heinze, J., Wurm, Y., Economou, C.K., Chapuisat, M., et al. (2022). Convergent evolution of a labile nutritional symbiosis in ants. *ISME J.* *16*, 2114–2122.
76. Van Leuven, J.T., Meister, R.C., Simon, C., and McCutcheon, J.P. (2014). Sympatric speciation in a bacterial endosymbiont results in two genomes with the functionality of one. *Cell* *158*, 1270–1280.
77. Berasategui, A., Salem, H., Paetz, C., Santoro, M., Gershenzon, J., Kaltenpoth, M., and Schmidt, A. (2017). Gut microbiota of the pine weevil degrades conifer diterpenes and increases insect fitness. *Mol. Ecol.* *26*, 4099–4110.
78. Ceja-Navarro, J.A., Vega, F.E., Karaoz, U., Hao, Z., Jenkins, S., Lim, H.C., Kosina, P., Infante, F., Northen, T.R., and Brodie, E.L. (2015). Gut microbiota mediate caffeine detoxification in the primary insect pest of coffee. *Nat. Commun.* *6*, 7618.
79. Sato, Y., Jang, S., Takeshita, K., Itoh, H., Koike, H., Tago, K., Hayatsu, M., Hori, T., and Kikuchi, Y. (2021). Insecticide resistance by a host-symbiont reciprocal detoxification. *Nat. Commun.* *12*, 6432.
80. Moran, N.A. (2007). Symbiosis as an adaptive process and source of phenotypic complexity. *Proc. Natl. Acad. Sci. USA* *104 (Suppl 1)*, 8627–8633.
81. Bolger, A.M., Lohse, M., and Usadel, B. (2014). Trimmomatic: a flexible trimmer for Illumina sequence data. *Bioinformatics* *30*, 2114–2120.
82. Li, D., Liu, C.M., Luo, R., Sadakane, K., and Lam, T.W. (2015). MEGAHIT: an ultra-fast single-node solution for large and complex metagenomics assembly via succinct de Bruijn graph. *Bioinformatics* *31*, 1674–1676.

83. Alneberg, J., Bjarnason, B.S., de Bruijn, I., Schirmer, M., Quick, J., Ijaz, U.Z., Lahti, L., Loman, N.J., Andersson, A.F., and Quince, C. (2014). Binning metagenomic contigs by coverage and composition. *Nat. Methods* **11**, 1144–1146.
84. Rissman, A.I., Mau, B., Biehl, B.S., Darling, A.E., Glasner, J.D., and Perna, N.T. (2009). Reordering contigs of draft genomes using the Mauve aligner. *Bioinformatics* **25**, 2071–2073.
85. Brown, C.T., Olm, M.R., Thomas, B.C., and Banfield, J.F. (2016). Measurement of bacterial replication rates in microbial communities. *Nat. Biotechnol.* **34**, 1256–1263.
86. Seemann, T. (2014). Prokka: rapid prokaryotic genome annotation. *Bioinformatics* **30**, 2068–2069.
87. Delcher, A.L., Bratke, K.A., Powers, E.C., and Salzberg, S.L. (2007). Identifying bacterial genes and endosymbiont DNA with Glimmer. *Bioinformatics* **23**, 673–679.
88. Syberg-Olsen, M.J., Garber, A.I., Keeling, P.J., McCutcheon, J.P., and Husnik, F. (2022). Pseudofinder: Detection of Pseudogenes in Prokaryotic Genomes. *Mol. Biol. Evol.* **39**, msac153.
89. Buchfink, B., Xie, C., and Huson, D.H. (2015). Fast and sensitive protein alignment using DIAMOND. *Nat. Methods* **12**, 59–60.
90. R Core Team (2019). R: A Language and Environment for Statistical Computing (R Foundation for Statistical Computing).
91. Wang, Y., Tang, H., Debary, J.D., Tan, X., Li, J., Wang, X., Lee, T.H., Jin, H., Marler, B., Guo, H., et al. (2012). MScanX: a toolkit for detection and evolutionary analysis of gene synteny and collinearity. *Nucleic Acids Res.* **40**, e49.
92. Bandi, V., and Gutwin, C. (2020). Interactive exploration of genomic conservation. In *Graphics Interface 2020*, pp. 74–83.
93. Conway, J.R., Lex, A., and Gehlenborg, N. (2017). UpSetR: an R package for the visualization of intersecting sets and their properties. *Bioinformatics* **33**, 2938–2940.
94. Gu, Z., Eils, R., and Schlesner, M. (2016). Complex heatmaps reveal patterns and correlations in multidimensional genomic data. *Bioinformatics* **32**, 2847–2849.
95. Edgar, R.C. (2004). MUSCLE: multiple sequence alignment with high accuracy and high throughput. *Nucleic Acids Res.* **32**, 1792–1797.
96. Ronquist, F., Teslenko, M., van der Mark, P., Ayres, D.L., Darling, A., Höhna, S., Larget, B., Liu, L., Suchard, M.A., and Huelsenbeck, J.P. (2012). MrBayes 3.2: efficient Bayesian phylogenetic inference and model choice across a large model space. *Syst. Biol.* **61**, 539–542.
97. Kozlov, A.M., Darriba, D., Flouri, T., Morel, B., and Stamatakis, A. (2019). RAxML-NG: a fast, scalable and user-friendly tool for maximum likelihood phylogenetic inference. *Bioinformatics* **35**, 4453–4455.
98. Lanfear, R., Frandsen, P.B., Wright, A.M., Senfeld, T., and Calcott, B. (2017). PartitionFinder 2: New methods for selecting partitioned models of evolution for molecular and morphological phylogenetic analyses. *Mol. Biol. Evol.* **34**, 772–773.
99. Suyama, M., Torrents, D., and Bork, P. (2006). PAL2NAL: robust conversion of protein sequence alignments into the corresponding codon alignments. *Nucleic Acids Res.* **34**, W609–W612.
100. Bernt, M., Donath, A., Jühling, F., Externbrink, F., Florentz, C., Fritsch, G., Pütz, J., Middendorf, M., and Stadler, P.F. (2013). MITOS: improved de novo metazoan mitochondrial genome annotation. *Mol. Phylogenet. Evol.* **69**, 313–319.
101. Bouckaert, R., Heled, J., Kühnert, D., Vaughan, T., Wu, C.H., Xie, D., Suchard, M.A., Rambaut, A., and Drummond, A.J. (2014). BEAST 2: a software platform for Bayesian evolutionary analysis. *PLoS Comput. Biol.* **10**, e1003537.
102. Venables, W.N., and Ripley, B.D. (2002). *Modern Applied Statistics with S*. In *Statistics and Computing* (Springer).
103. Santichaivekin, S., Yang, Q., Liu, J., Mawhorter, R., Jiang, J., Wesley, T., Wu, Y.C., and Libeskind-Hadas, R. (2021). eMPress: a systematic co-phylogeny reconciliation tool. *Bioinformatics* **37**, 2481–2482.
104. Liao, Y., Smyth, G.K., and Shi, W. (2014). featureCounts: an efficient general purpose program for assigning sequence reads to genomic features. *Bioinformatics* **30**, 923–930.
105. Love, M.I., Huber, W., and Anders, S. (2014). Moderated estimation of fold change and dispersion for RNA-seq data with DESeq2. *Genome Biol.* **15**, 550.
106. Kolde, R., and Kolde, M.R. (2015). Package ‘pheatmap’. R package **1**, 790.
107. Hothorn, T., Bretz, F., and Westfall, P. (2008). Simultaneous inference in general parametric models. *Biom. J.* **50**, 346–363.
108. Stanke, M., Keller, O., Gunduz, I., Hayes, A., Waack, S., and Morgenstern, B. (2006). AUGUSTUS: ab initio prediction of alternative transcripts. *Nucleic Acids Res.* **34**, W435–W439.
109. Haas, B.J., Papanicolaou, A., Yassour, M., Grabherr, M., Blood, P.D., Bowden, J., Couger, M.B., Eccles, D., Li, B., Lieber, M., et al. (2013). De novo transcript sequence reconstruction from RNA-seq using the Trinity platform for reference generation and analysis. *Nat. Protoc.* **8**, 1494–1512.
110. Simão, F.A., Waterhouse, R.M., Ioannidis, P., Kriventseva, E.V., and Zdobnov, E.M. (2015). BUSCO: assessing genome assembly and annotation completeness with single-copy orthologs. *Bioinformatics* **31**, 3210–3212.
111. Kriventseva, E.V., Kuznetsov, D., Tegenfeldt, F., Manni, M., Dias, R., Simão, F.A., and Zdobnov, E.M. (2019). OrthoDB v10: sampling the diversity of animal, plant, fungal, protist, bacterial and viral genomes for evolutionary and functional annotations of orthologs. *Nucleic Acids Res.* **47**, D807–D811.
112. Haas, B., and Papanicolaou, A. (2013). TransDecoder (find coding regions within transcripts). [GitHub. https://github.com/TransDecoder/transdecoder.github.io/blob/master/index.asciidoc](https://github.com/TransDecoder/transdecoder.github.io/blob/master/index.asciidoc).
113. Edger, P.P., Heide-Fischer, H.M., Bekaert, M., Rota, J., Glöckner, G., Platts, A.E., Heckel, D.G., Der, J.P., Wafula, E.K., Tang, M., et al. (2015). The butterfly plant arms-race escalated by gene and genome duplications. *Proc. Natl. Acad. Sci. USA* **112**, 8362–8366.
114. Chen, L.X., Anantharaman, K., Shaiber, A., Eren, A.M., and Banfield, J.F. (2020). Accurate and complete genomes from metagenomes. *Genome Res.* **30**, 315–333.
115. Shaiber, A., Willis, A.D., Delmont, T.O., Roux, S., Chen, L.X., Schmid, A.C., Yousef, M., Watson, A.R., Lolans, K., Esen, Ö.C., et al. (2020). Functional and genetic markers of niche partitioning among enigmatic members of the human oral microbiome. *Genome Biol.* **21**, 292.
116. Sokal, R.R., and Rohlf, F.J. (1994). *Biometry: The Principles and Practice of Statistics in Biological Research*, Third Edition (WH Freeman and Co.).
117. Berasategui, A., Breitenbach, N., García-Lozano, M., Pons, I., Sailer, B., Lanz, C., Rodríguez, V., Hipp, K., Ziemert, N., Windsor, D., et al. (2022). The leaf beetle *Chelymormpha alternans* propagates a plant pathogen in exchange for pupal protection. *Curr. Biol.* **32**, 4114–4127.e6.
118. Langmead, B., and Salzberg, S.L. (2012). Fast gapped-read alignment with Bowtie 2. *Nat. Methods* **9**, 357–359.
119. Cheng, H., Concepcion, G.T., Feng, X., Zhang, H., and Li, H. (2021). Haplotype-resolved de novo assembly using phased assembly graphs with hifiasm. *Nat. Methods* **18**, 170–175.
120. Zhang, H., Yohe, T., Huang, L., Entwistle, S., Wu, P., Yang, Z., Busk, P.K., Xu, Y., and Yin, Y. (2018). dbCAN2: a meta server for automated carbohydrate-active enzyme annotation. *Nucleic Acids Res.* **46**, W95–W101.
121. Signorell, A., Aho, K., Alfons, A., Anderegg, N., and Aragon, T. (2024). DescTools: Tools for descriptive statistics. R package version 0.99.

STAR★METHODS

KEY RESOURCES TABLE

REAGENT or RESOURCE	SOURCE	IDENTIFIER
Bacterial and virus strains		
<i>Candidatus</i> <i>Stammera capleta</i>	This study and Salem et al. ³ Salem et al. ⁴ Pons et al. ⁷	NCBI Taxonomy ID: 2608262
Biological samples		
<i>Alurnus ornatus</i> collected in Panama	This study	Tribe: Alurnini
<i>Arescus</i> sp. collected in Panama	This study	Tribe: Arescini
<i>Chelobasis bicolor</i> collected in Panama	This study	Tribe: Arescini
<i>Chelobasis perplexa</i> collected in Panama	This study	Tribe: Arescini
<i>Aspidimorpha madagascarica</i> collected in La Reunion, France	This study	Tribe: Aspidimorphini
<i>Aspidimorpha quinquefasciata</i> collected in La Reunion, France	This study	Tribe: Aspidimorphini
<i>Agroiconota Judaica</i>	This study	Tribe: Cassidini
<i>Agroiconota propinqua</i> collected in Panama	Salem et al. ⁴	Tribe: Cassidini
<i>Cassida murraea</i> collected in Germany	This study	Tribe: Cassidini
<i>Cassida rubiginosa</i> collected in New Zealand	Salem et al. ³	Tribe: Cassidini
<i>Cassida versicolor</i> collected in Germany	Salem et al. ⁴	Tribe: Cassidini
<i>Cassida vibex</i> collected in Germany	Salem et al. ⁴	Tribe: Cassidini
<i>Cassida viridis</i> collected in Germany	Salem et al. ⁴	Tribe: Cassidini
<i>Charidotella egregia</i> collected in Panama	This study	Tribe: Cassidini
<i>Charidotella sexpunctata</i> collected in USA	Salem et al. ⁴	Tribe: Cassidini
<i>Charidotella</i> sp. collected in Martinique, France	This study	Tribe: Cassidini
<i>Charidotella subannulata</i> collected in Panama	This study	Tribe: Cassidini
<i>Charidotella tuberculata</i> collected in Panama	This study	Tribe: Cassidini
<i>Charidotella zona</i> collected in Panama	This study	Tribe: Cassidini
<i>Charidotus auropunctata</i> collected in Panama	This study	Tribe: Cassidini
<i>Charidotus inctincta</i> collected in Panama	This study	Tribe: Cassidini
<i>Deloyala guttata</i> collected in Panama	This study	Tribe: Cassidini
<i>Ischnocodia annulus</i> collected in Panama	Salem et al. ⁴	Tribe: Cassidini
<i>Microctenochira fraterna</i> collected in Panama	This study	Tribe: Cassidini
<i>Microctenochira panamensis</i> collected in Panama	This study	Tribe: Cassidini
<i>Microctenochira</i> sp. collected in Panama	This study	Tribe: Cassidini
<i>Microctenochira tabida</i> collected in Panama	This study	Tribe: Cassidini
<i>Parachiridia semiannulata</i> collected in Panama	Salem et al. ⁴	Tribe: Cassidini
<i>Parachiridia subirrorata</i> collected in Panama	This study	Tribe: Cassidini
<i>Plagiometriona latimarginata</i> collected in Panama	This study	Tribe: Cassidini
<i>Xenocassis ambita</i> collected in Panama	This study	Tribe: Cassidini
<i>Microrhopala vittata</i> collected in Panama	This study	Tribe: Chalepini
<i>Oxychalepus posticatus</i> collected in Panama	This study	Tribe: Chalepini
<i>Physonota</i> sp. collected in Panama	This study	Tribe: Goniochenini
<i>Polychalma multicava</i> collected in Panama	This study	Tribe: Goniochenini
<i>Cistudinella foveolata</i> collected in Panama	Salem et al. ⁴	Tribe: Ischyrosomychni
<i>Acromis sparsa</i> collected in Panama	Salem et al. ⁴	Tribe: Mesomphaliini
<i>Chelymorpha alternans</i> collected in Germany	This study	Tribe: Mesomphaliini

(Continued on next page)

Continued

REAGENT or RESOURCE	SOURCE	IDENTIFIER
<i>Chelymopha bullata</i> collected in Panama	This study	Tribe: Mesomphaliini
<i>Chelymopha cassidea</i> collected in USA	This study	Tribe: Mesomphaliini
<i>Chelymopha gressoria</i> collected in Panama	This study	Tribe: Mesomphaliini
<i>Stolas discoides</i> collected in Panama	Salem et al. ⁴	Tribe: Mesomphaliini
<i>Stolas variability</i> collected in Panama	This study	Tribe: Mesomphaliini
<i>Terpsis quadrimaculatta</i> collected in Panama	This study	Tribe: Mesomphaliini
<i>Notosacantha ihai</i> collected in Japan	This study	Tribe: Notosacanthini
<i>Discomorpha panamensis</i> collected in Panama	Salem et al. ⁴	Tribe: Omocerini
<i>Discomorpha sp.</i> collected in Panama	This study	Tribe: Omocerini
<i>Prosopodonta dorsata</i> collected in Panama	This study	Tribe: Prosopodontini
<i>Prosopodonta limbata</i> collected in Panama	This study	Tribe: Prosopodontini
<i>Sceloenopla sp.</i> collected in Panama	This study	Tribe: Spilophorini
<i>Calyptocephala attenuata</i> collected in Panama	This study	Tribe: Spilophorini
<i>Calyptocephala gerstaeckeri</i> collected in Panama	This study	Tribe: Spilophorini
<i>Spilophoroides marginatus</i> collected in Panama	This study	Tribe: Spilophorini
<i>Spilophora sp.</i> collected in Panama	This study	Tribe: Spilophorini
<i>Spilophora sp.</i> collected in Panama	This study	Tribe: Spilophorini

Chemicals, peptides, and recombinant proteins

Polygalacturonic acid	Sigma-Aldrich	Cat#81325
Pectinase (<i>Aspergillus niger</i>)	Sigma-Aldrich	Cat#P4716
TLC plates Silica gel 60	Merck	Cat#116835
Galacturonic acid monohydrate	Sigma-Aldrich	Cat#92478
Di-galacturonic acid	Sigma-Aldrich	Cat#D4288
Tri-galacturonic acid	Sigma-Aldrich	Cat#7407
Glucomanan	Megazyme	Cat#P-GLCML
endo-1,4-beta-Mannanase (<i>Aspergillus niger</i>)	Megazyme	Cat#E-BMANN
Mannose	Sigma-Aldrich	Cat#92683
Mannobiose	Megazyme	Cat#O-MBI
Mannotriose	Megazyme	Cat#O-MTR
Mannotetraose	Megazyme	Cat#O-MTE
Roti®-Histol	Carl Roth	Cat#6640.1
Paraplast High Melt	Leica	Cat#39601095
ProLong® Gold Antifade Mountant	Thermo Scientific	Cat#P36930
DAPI	Carl Roth	Cat#6335.1

Critical commercial assays

Qubit™ dsDNA HS Assay Kit	Thermo Fisher	Cat#Q32854
SPRI beads	Beckman Coulter	Cat#B23318
NEBNext® Ultra™ II DNA Library Prep Kit for Illumina	New England Biolabs	Cat#E7645
NEBNext Multiplex Oligos for Illumina (Index Primer Set 1)	New England Biolabs	Cat#E7335
NEBNext Multiplex Oligos for Illumina (Index Primer Set 2)	New England Biolabs	Cat#E7500
NEBNext Multiplex Oligos for Illumina (Index Primer Set 3)	New England Biolabs	Cat#E7710
QIAGEN RNeasy Mini Kit	Qiagen	Cat#74106
Qubit™ RNA High Sensitivity (HS) kit	Thermo Fisher	Cat#Q32852
NEBNext® rRNA Depletion Kit (Human/Mouse/Rat)	New England Biolabs	Cat#E7405
NEBNext® Ultra™ Directional II RNA Library Prep	New England Biolabs	Cat#7760
Agilent Technologies High Sensitivity DNA Kit	Agilent	Cat#5067-4626
QIAGEN DNeasy Blood & Tissue Kit	Qiagen	Cat#69506
Platinum SYBR Green qPCR SuperMix-UDG	Thermo Scientific	Cat#11744100
Monarch HMW DNA extraction Kit	New England Biolabs	Cat#T3060

(Continued on next page)

Continued

REAGENT or RESOURCE	SOURCE	IDENTIFIER
SMRTbell Express Template Prep Kit 2.0	Pacific Bioscience	Cat#100-938-900
AMPure PB Beads	Pacific Bioscience	Cat#100-265-900
SMRTbell Enzyme Clean Up Kit 2.0	Pacific Bioscience	Cat#101-932-600
Sequencing Primer v5	Pacific Bioscience	Cat#102-067-400
BluePippin System 0.75% Agarose Cassettes, Marker S1	Sage Science	Cat#BLU0001
Sequel II Binding Kit 2.2	Pacific Bioscience	Cat#101-894-200
Sequel II Sequencing Kit 2.0	Pacific Bioscience	Cat#101-820-200
SMRT Cell 8M Tray	Pacific Bioscience	Cat#101-389-001
NEBNext® Poly(A) mRNA Magnetic Isolation Module	New England Biolabs	Cat#E74905

Deposited data

Genomic, metagenomic and transcriptomic data	This study	NCBI:PRJNA947801
<i>Agroiconota propinqua</i>	Salem et al. ⁴	SRA:SRX6755582
<i>Cassida rubiginosa</i>	Salem et al. ³	SRA:SRX3259630;SRR6176960
<i>Cassida versicolor</i>	Salem et al. ⁴	SRA:SRX6755584
<i>Cassida vibex</i>	Salem et al. ⁴	SRA:SRX6755581
<i>Cassida viridis</i>	Salem et al. ⁴	SRA:SRX6755580
<i>Charidotella sexpunctata</i>	Salem et al. ⁴	SRA:SRX6755583
<i>Ichnocodia annulus</i>	Salem et al. ⁴	SRA:SRX6755586;SRR10030203
<i>Parachiridia semiannulata</i>	Salem et al. ⁴	SRA:SRX6755585;SRR10030204
<i>Cistudinella foveolata</i>	Salem et al. ⁴	SRA:SRX6755590;SRR10030206
<i>Acromis sparsa</i>	Salem et al. ⁴	SRA:SRX6755589;SRR10030202
<i>Chelymorpha alternans</i>	Salem et al. ⁴	SRA:SRX6755588;SRR10030205
<i>Stolas discoides</i>	Salem et al. ⁴	SRA:SRX6755587
<i>Discomorpha panamensis</i>	Salem et al. ⁴	SRA:SRX6755591;SRR10030201
Blochmannia endosymbiont of <i>Camponotus modoc</i>	NCBI	RefSeq:GCF_023585785.1
<i>Buchnera aphidicola</i>	NCBI	RefSeq:GCF_003099975.1
<i>Candidatus</i> Hamiltonella defensa	NCBI	RefSeq:GCF_000021705.1
<i>Candidatus</i> Ishikawaella capsulata Mpkobe	NCBI	RefSeq:GCF_000828515.1
<i>Candidatus</i> Moranella endobia	NCBI	RefSeq:GCF_000364725.1
<i>Candidatus</i> Regiella insecticola	NCBI	RefSeq:GCF_013373955.1
<i>Candidatus</i> Sodalis pierantonius str. SOPE	NCBI	RefSeq:GCF_000517405.1
<i>Citrobacter koseri</i>	NCBI	RefSeq:GCF_000018045.1
<i>Enterobacter mori</i>	NCBI	RefSeq:GCF_022014715.1
<i>Erwinia tasamniensis</i>	NCBI	RefSeq:GCF_000026185.1
<i>Escherichia coli</i>	NCBI	RefSeq:GCF_000005845.2
<i>Haemophilus influenzae</i>	NCBI	RefSeq:GCF_000931575.1
<i>Klebsiella pneumoniae</i>	NCBI	RefSeq:GCF_000240185.2
<i>Pantoea vagans</i>	NCBI	RefSeq:GCF_004792415.1
<i>Pasteurella multocida</i>	NCBI	RefSeq:GCF_002073255.2
<i>Pectobacterium caratovora</i>	NCBI	RefSeq:GCF_013488025.1
<i>Photorhabdus luminescens</i>	NCBI	RefSeq:GCF_001083805.1
<i>Proteus mirabilis</i>	NCBI	RefSeq:GCF_000069965.1
<i>Pseudomonas entomophila</i>	NCBI	RefSeq:GCF_000026105.1
<i>Salmonella typhimurium</i>	NCBI	RefSeq:GCF_000006945.2
<i>Serratia symbiotica</i>	NCBI	RefSeq:GCF_009831665.3
<i>Vibrio fischeri</i>	NCBI	RefSeq:GCF_000020845.1
<i>Xanthomonas campestris</i>	NCBI	RefSeq:GCF_013388375.1
<i>Xenorhabdus nematophila</i>	NCBI	RefSeq:GCF_014295015.1
<i>Xylella fastidiosa</i>	NCBI	RefSeq:GCF_000007245.1
<i>Yersinia pestis</i>	NCBI	RefSeq:GCF_024498375.1

(Continued on next page)

Continued

REAGENT or RESOURCE	SOURCE	IDENTIFIER
Experimental models: Organisms/strains		
<i>Chelymorpha alternans</i> maintained at the Max Planck Institute for Biology	This study	N/A
Oligonucleotides		
Primer polygalacturonase <i>Stammera</i> :pg1_Chely_qpcr_F: AGCATCAAATGGACCTACATCACAA	This study	Plasmid from <i>Stammera</i> of <i>Chelymorpha alternans</i>
Primer polygalacturonase <i>Stammera</i> :pg1_Chely_qpcr_R: ACCACTAGTTGTTCCGTTTCATTGA	This study	Plasmid from <i>Stammera</i> of <i>Chelymorpha alternans</i>
Primer 60 kDa chaperonin <i>Stammera</i> : groL1_Chely_qpcr_F: TGCTGCTTCTGTTGCTGGAT	This study	Chromosome from <i>Stammera</i> of <i>Chelymorpha alternans</i>
Primer 60 kDa chaperonin <i>Stammera</i> : groL1_Chely_qpcr_R: TTCCACCCATTCTGAACCA	This study	Chromosome from <i>Stammera</i> of <i>Chelymorpha alternans</i>
Primer 16S ribosomal RNA <i>Stammera</i> : f16S_StaChe: CGAGGGATGCGAGCGTTAAT	Pons et al. ⁷	Chromosome from <i>Stammera</i> of <i>Chelymorpha alternans</i>
Primer 16S ribosomal RNA <i>Stammera</i> : r16S_StaChe: CCGCCCTTCGCCACTGATATT	Pons et al. ⁷	Chromosome from <i>Stammera</i> of <i>Chelymorpha alternans</i>
Primer for polygalacturonase in <i>Calyptocephala attenuata</i> pg1_Caly_F: TGTGTAGTGTGTCATTTCCGG	This study	Polygalacturonase encoded by <i>Calyptocephala attenuata</i>
Primer for polygalacturonase in <i>Calyptocephala attenuata</i> pg1_Caly_R: TTTGCCAGCGTGAGTAATGA	This study	Polygalacturonase encoded by <i>Calyptocephala attenuata</i>
FISH probe 18S ribosomal RNA: EUK1195: GGGCATCACAGACCTG	N/A	All eukaryotes
FISH probe 16S ribosomal RNA: SCA600: AAACCACCTACATGCTCTTTACGCC	This study	<i>Stammera</i> from 52 Cassidinae species
FISH probe 16S ribosomal RNA: SAL227: GGTCTTGAAAAAAAAGATCCCC	This study	<i>Stammera</i> from <i>Chelymorpha alternans</i>
Software and algorithms		
Trimmomatic	Bolger et al. ⁸¹	http://www.usadellab.org/cms/?page=trimmomatic
MEGAHIT	Li et al. ⁸²	https://github.com/voutcn/megahit
CONCOCT	Alneberg et al. ⁸³	https://github.com/BinPro/CONCOCT
Mauve aligner	⁸⁴	https://darlinglab.org/mauve/mauve.html
Geneious Prime	N/A	https://www.geneious.com/
iRep	Brown et al. ⁸⁵	https://github.com/christophertbrown/iRep
Prokka v1.14.6	Seemann ⁸⁶	https://github.com/tseemann/prokka
Glimmer	Delcher et al. ⁸⁷	https://ccb.jhu.edu/software/glimmer/index.shtml
Pseudofinder	Syberg-Olsen et al. ⁸⁸	https://github.com/filip-husnik/pseudofinder
anvi'o v8.1-dev	Eren et al. ³⁰	https://anvio.org/
DIAMOND	Buchfink et al. ⁸⁹	https://github.com/bbuchfink/diamond
R	R Core Team ⁹⁰	https://www.r-project.org/
MCSanX	Wang et al. ⁹¹	https://github.com/wyp1125/MCSanX
SynVisio	Bandi et al. ⁹²	https://synvisio.github.io/#/
UpSet R package	Conway et al. ⁹³	https://github.com/hms-dbmi/UpSetR
ComplexHeatmap R package	Gu et al. ⁹⁴	https://github.com/jokergoo/ComplexHeatmap
MUSCLE	Edgar ⁹⁵	https://www.drive5.com/muscle/

(Continued on next page)

Continued

REAGENT or RESOURCE	SOURCE	IDENTIFIER
MrBayes (v3.2.7a)	Ronquist et al. ⁹⁶	https://nbisweden.github.io/MrBayes/
RAxML-NG	Kozlov et al. ⁹⁷	https://github.com/amkozlov/raxml-ng
PartitionFinder2	Lanfear et al. ⁹⁸	https://www.robertlanfear.com/partitionfinder/
PAL2NAL (v14)	Suyama et al. ⁹⁹	https://www.bork.embl.de/pal2nal/
PAML (v4.9)	Yang ³⁸	http://abacus.gene.ucl.ac.uk/software/paml.html
Mesquite (v.3.7)	Maddison et al. ⁴²	https://www.mesquiteproject.org/
MITOS2 webserver	Bernt et al. ¹⁰⁰	http://mitos.bioinf.uni-leipzig.de/
BEAST2 (v2.4.8)	Bouckaert et al. ¹⁰¹	https://www.beast2.org/
DescTools R package	Signorell et al. ¹⁰²	https://cran.r-project.org/web/packages/DescTools/index.html
eMPress GUI	Santichaivekin et al. ¹⁰³	https://sites.google.com/g.hmc.edu/empress/home/gui
MEDUSA	Brown et al. ⁷¹	https://github.com/josephwb/turboMEDUSA
bowtie2 (v2.3.5.1)	Langmead et al. ¹⁰⁴	https://github.com/BenLangmead/bowtie2
featureCounts	Liao et al. ¹⁰⁵	https://subread.sourceforge.net/
DESeq2 R package	Love et al. ¹⁰⁶	https://bioconductor.org/packages/release/bioc/html/DESeq2.html
pheatmap R package	Kolde et al. ⁹⁰	https://github.com/raivokolde/pheatmap
MASS R package	Venables et al. ¹⁰⁷	https://cran.r-project.org/web/packages/MASS/index.html
Multcomp R package	N/A	https://cran.r-project.org/web/packages/multcomp/index.html
Hifiasm (v0.14.1-r314)	Cheng et al. ¹⁰⁸	https://github.com/chhylp123/hifiasm
AUGUSTUS	Stanke et al. ¹⁰⁹	https://github.com/Gaius-Augustus/Augustus
Trinity platform (v2.8.5)	Haas et al. ¹¹⁰	https://github.com/trinityrnaseq/trinityrnaseq
BUSCO (v5.1.2)	Simão et al. ¹¹¹	https://busco.ezlab.org/
TransDecoder (v5.5.0)	Haas et al. ¹¹²	https://github.com/TransDecoder/TransDecoder
run_dbcan	Zhang et al. ¹¹³	https://github.com/linnabrown/run_dbcan

RESOURCE AVAILABILITY

Lead contact

Further information and requests for resources and commercial reagents should be directed to and will be fulfilled by the lead contact, Hassan Salem (hassan.salem@tuebingen.mpg.de).

Materials availability

This study did not generate new unique reagents.

Data and code availability

Genomic, metagenomic and transcriptomic sequencing data generated in this study have been deposited at the National Center for Biotechnology Information (NCBI) and are publicly available as of the date of publication under BioProject PRJNA947801.

This paper does not report original code. Any additional information required to reanalyze the data reported in this paper is available from the [lead contact](#) upon request.

EXPERIMENTAL MODEL AND STUDY PARTICIPANT DETAILS

Adult Cassidinae species were collected in France, Germany, Japan, New Zealand, Panama, and the United States of America between 2018–2023. For DNA sequencing, insects were submerged in molecular grade 99% ethanol after collection and kept at -20°C

for further processing. *Calyptocephala attenuata* and *Chelobasis bicolor* were snap frozen in liquid nitrogen ahead of RNA extraction and transcriptome sequencing. *C. bicolor* was also used for enzymatic assays, along with *Chelymorpha alternans*, which are continuously reared at the Max Planck Institute for Biology (Tübingen, Germany) in climate chambers at a constant temperature of 26°C, humidity of 60% and long light regimes (14.30 h/9.30 h light/dark cycles). The latter species was also used to study *Stammera*'s gene expression across different host developmental stages and compartments. All experiments were performed in accordance with relevant guidelines and are in compliance with EU and German legislation on insect rearing and experimentation.

METHOD DETAILS

Genome sequencing and assembly

Metagenomic sequencing was performed across 55 representative Cassidinae beetle species and spanning 13 tribes. 42 of these species were collected in this study and dissections were performed using 1–3 individuals under molecular grade 99% ethanol. DNA was extracted using the QIAGEN DNeasy Blood & Tissue Kit with RNase treatment. Genomic DNA was fragmented to an average size of 300 bp using Covaris S2. Sheared DNA was purified by SPRI beads and used to construct DNaseq libraries using the NEBNext® Ultra™ II DNA Library Prep Kit for Illumina. 12 libraries were sequenced on an Illumina HiSeq 3000 system, and due to an update of Illumina sequencing technologies at the institute, 30 libraries were sequenced on an Illumina NextSeq 2000 system at the Max Planck for Biology (Tübingen, Germany) using the paired-end 150 bp technology with a depth of ~50 million reads.

Adaptor removal and quality filtering of raw reads was performed by Trimmomatic (v0.36).⁸¹ Metagenomic sequences of 42 Cassidinae species generated in this study in addition to 13 publicly available Cassidinae sequencing read sets⁴ were *de novo* assembled by MEGAHIT.⁸² Contigs belonging to *Stammera* were binned according to coverage and GC content by CONCOCT.⁸³ Out of the 50 *Stammera* genomes, 27 were automatically assembled into a single chromosomal sequence, while the other 23 consisted of 2 to 8 contigs. These contigs were reordered and scaffolded by comparing them to a complete *Stammera* assembly from the same host genus using the Mauve Aligner.⁸⁴ Subsequently, genome curation procedures, involving the filling of scaffolding gaps in the 23 fragmented genomes and the removal of local assembly errors in all 50 genomes, were carried out following established protocols.¹¹⁴

After verification of complete single-chromosomal *Stammera* genomes, GC skew was calculated by iRep⁸⁵ to identify the origin of replication. OriC sites were then set in Geneious Prime 2019.2.3 (<https://www.geneious.com>).

Stammera comparative genomics

Symbiont genome annotation

Symbiont protein-coding genes were predicted by Prodigal as implemented in Prokka (v1.14.6)⁸⁶ using the genetic code 4 (TGA encoding tryptophan) as described by Salem et al.⁴ Additional gene predictions were performed by Glimmer⁸⁷ and a manual curation of annotation files was performed to consolidate the gene predictions. tRNAs, rRNAs and ncRNAs were predicted by ARAGORN, Barrnap and Infernal as implemented in Prokka (v1.14.6).⁸⁶ Pseudogenes were predicted in each genome using Pseudofinder.⁸⁸

Pangenome analysis

Pfam, KOfam, NCBI COG's, and KEGG annotations were additionally included in anvi'o (v8.1-dev).³⁰ Subsequently, a pangenome analysis of 50 *Stammera* genomes was performed (minbit= 0.3, MCL inflation parameter=2) using DIAMOND⁸⁹ for amino acid sequence similarity search (--sensitive).³⁰ Orthologous genes were considered part of the core genome if present in 100% of the genomes (a total of 50). Accessory genes were designated as gene clusters present in at least one *Stammera* genome but not in more than 49 genomes. Singletons were defined as genes exclusive to a single *Stammera* genome. anvi-compute-functional-enrichment-in-pan program,¹¹⁵ as implemented in anvi'o, was used to identify enriched functions in *Stammera* from tortoise and hispine beetles.

Conservation of gene order in *Stammera* genomes was assessed by MCScanX, including a representative of each tribe,⁹¹ and the results were visualized in SynVisio.⁹² Distribution of gene clusters across *Stammera* from tortoise and hispine beetles was visualized by an Upset plot based on a presence/absence matrix obtained from *Stammera*'s pangenome. This plot was constructed using the R packages UpSet⁹³ and ComplexHeatmap.⁹⁴ A pangenome with functions was obtained with the program anvi-display-functions in anvi'o to compare gene functions rather than gene sequences across *Stammera* genomes, resulting in a frequency and a presence/absence table of COG categories.

Symbiont phylogenetic reconstruction

124 single-copy core genes identified by anvi'o were extracted from each *Stammera* genome and individually aligned using MUSCLE (v3.8.1551).⁹⁵ Unrooted phylogenies encompassing the 50 *Stammera* taxa were constructed from a concatenated multigene alignment by Bayesian and Maximum Likelihood (ML) methods using MrBayes (v3.2.7a)⁹⁶ (ngen=1000000, samplefreq=1000) and RAXML-NG (v1.2.0)⁹⁷ (ngen=1000), respectively. Concatenated alignments of 61 single-copy genes present in all *Stammera* taxa, and 26 outgroups indicated in the [key resources table](#), were included to construct Bayesian and ML phylogenies using *Xanthomonas campestris* as a root (Figure S1). The best-fit substitution models for each analysis were selected using PartitionFinder2⁹⁸ (branchlengths=unlinked, models = all, model_selection = bic).

Stammera molecular evolution

To determine the signatures of selection acting on *Stammera*'s genes, we measured rates of synonymous (dS) and nonsynonymous (dN) substitutions across core, orthologous single-copy genes. This parameter determines whether genes experience strong

purifying selection ($\omega < 0.1$), relaxed purifying selection ($1 < \omega > 0.1$), or positive selection ($\omega > 1$).³³ Codon-based alignments were performed for each gene in PAL2NAL (v14)⁹⁹ and by using the unrooted *Stammera* Bayesian tree. dN/dS ratios were estimated for each using codeml as implemented in PAML (v4.9)³⁸ by applying three models. The M0 model was used to test for selection across all codon sites. Additionally, the site-based model M1a (nearly neutral) allowing for two categories of sites ($\omega = 1$ and $\omega = 0$), was compared to the M2a model (positive selection) which allows an additional category of positively selected sites ($\omega > 1$). To test for sites with significant support for each model, Likelihood Ratio Tests (LRTs) were compared against X^2 .

Ancestral state reconstruction

Genes encoding for plant-cell wall digestive enzymes were identified in *Stammera*'s pangenome. Ancestral nodes of these genes were inferred in the unrooted Maximum Likelihood *Stammera* tree using the trace character history function as implemented in Mesquite (v.3.7).⁴² This phylogeny was rooted according to the *Stammera* tree that included the outgroup species indicated in the [key resources table](#). A category character matrix was created using a gene presence/absence table and likelihood calculations were performed using the Mk1 model. Ancestral nodes for each gene were identified in the symbiont tree using a cut-off likelihood value $> 50\%$.

Host phylogenetic reconstruction

Host mitochondrial genomes were extracted from metagenomic assemblies based on coverage and GC content. BLAST searches confirmed the insect origin of mitochondrial genomes and these were further annotated using the MITOS2 webserver (<http://mitos2.bioinf.uni-leipzig.de>).¹⁰⁰ A concatenated alignment of 15 mitochondrial genes (13 protein coding genes + 2 ribosomal rRNA genes) was partitioned to assign the most appropriate substitution model to each gene using PartitionFinder2. Phylogenetic analyses were performed using both Bayesian inference and Maximum Likelihood in MrBayes⁹⁶ (ngen=5000000, samplefreq=1000) and RAxML-NG⁹⁷ (n=1000), respectively (Figure S2). Members of Spilopyrinae and Eumolpinae subfamilies from the Chrysomelidae were used as outgroups for this analysis. Bayesian time calibrated phylogenies were inferred by BEAST2 (v2.4.8)¹⁰¹ using the generated partition scheme. Substitution models were selected by bModelTest as implemented in BEAST. The tree prior included the calibrated Yule Model with a random starting tree. Three internal node calibrations, Notosacanthini (47 Mya),⁶⁹ Chalepini (44.1 Mya),¹⁸ and, Cassidini (40 Mya),⁷⁰ were applied with a normal prior distribution. Multiple BEAST chains (ngen = 10000000) were run per genome alignment and sampled every 1000 generations with a strict clock mode.

Host-symbiont cophylogenetic analysis

The tree reconciliation software eMPress GUI¹⁰³ was used to study the evolutionary relationship between Cassidinae and *Stammera*. This software reconciles symbiont and host trees using the DuplicationTransfer-Loss (DTL) model. Host and symbiont Maximum Likelihood phylogenetic trees were used as input and the analysis was conducted using the following eMPress parameters: duplication cost = 1, transfer cost = 1, and loss cost = 1. The significance of reconciliation between host and symbiont tree was calculated by randomizing the tips of the branches and then, re-calculating the cost to reconcile the phylogenies. Congruent phylogenies are obtained when the original cost of reconciliation is less than expected by chance ($p < 0.01$).

Diversification rate analyses

We applied MEDUSA (Modeling Evolutionary Diversification Using Stepwise Akaike Information Criterion)⁷¹ to estimate shifts in the diversification of the Cassidinae relative to *Stammera* acquisition. For this analysis, we collapsed the time-calibrated Cassidinae phylogeny obtained from BEAST to incorporate tribe-level species estimates reported by Chaboo.¹⁷ As a complementary test, we compared species richness between non-symbiotic and symbiotic cassidines using the G-test of goodness-of-fit.¹¹⁶ We also investigated whether symbiotic beetles exploit greater diversity of plant families relative to non-symbiotic cassidines. Host-plant family assignments for each Cassidinae tribe was also accessed from Chaboo.¹⁷

Symbiont transcriptome sequencing

To characterize differences in symbiont gene expression relative to *Stammera* localization and host development, transcriptome sequencing of egg caplets, foregut symbiotic organs of 3rd instar *Chelymorpha alternans* larvae and 24-day-old adults was performed. Six egg clutches of ~ 30 eggs representing three replicates were first divided in half two days after oviposition. Caplets were removed with sterilized scissors from one of each half. Treatments were pooled, yielding 30 caplets in each replicate. The remaining eggs were maintained under standard growth conditions (26°C and 60% relative humidity) previously described in Pons et al.⁷ and Berasategui et al.¹¹⁷ Three larvae from each replicate were collected nine days after hatching. Foregut symbiotic organs were dissected from larvae using sterilized scissors. The remaining larvae were kept under the same conditions until reaching adulthood. Three female adults from each replicate were sampled 24 days after emergence and foregut symbiotic organs were dissected for further processing. RNA extraction was performed for each sample immediately after collection using the QIAGEN RNeasy Mini Kit according to the protocol 4: Enzymatic Lysis and Proteinase K Digestion of Bacteria starting from step 7. This protocol is included in the RNAprotect® Bacteria Reagent Handbook from Qiagen. Total RNA was further quantified using the Qubit™ RNA High Sensitivity (HS) kit. 30 ng of total RNA were used as input to prepare nine RNA sequencing libraries for egg caplets, foregut symbiotic organs of larvae, and foregut symbiotic organs of adults (3 biological replicates each). Due to sequence similarity, ribosomal RNA was depleted from total RNA using the NEBNext® rRNA Depletion Kit (Human/Mouse/Rat). Libraries were constructed using the

NEBNext® Ultra™ Directional II RNA Library Prep and their size was confirmed in a 2100 Bioanalyzer system using the Agilent Technologies High Sensitivity DNA Kit. Sequencing of final libraries was performed on an Illumina HiSeq 3000 system (2x150bp) at the Max Planck Institute for Biology (Tübingen, Germany) with a depth of 30 million reads.

Adapter removal and quality filtering of raw reads was performed in Trimmomatic.⁸¹ Filtered reads were mapped to *Stammera* genome using bowtie2 (v2.3.5.1)¹¹⁸ (--fr, --no-unal). Gene counts were summarized using the featureCounts program¹⁰⁴ (--p, --countReadPairs, --s 2) as part of the Subread package release 2.0.0. Read counts were normalized by the DESeq2's median of ratios as established in the DESeq2¹⁰⁵ package in R. A heatmap of the log(x+1) normalized reads was then constructed using the pheatmap package¹⁰⁶ to visualize the expression profile across samples. Global transcriptome profile between samples was compared by testing for significant clusters using a permuted multivariate analysis of variance (PERMANOVA) using the vegan::adonis() function in R v.4.3.1.⁹⁰ The likelihood ratio test (LRT), implemented in DESeq2, was used to test for differences in symbiont gene expression across egg caplets and foregut-symbiotic organs of larvae and adults. Differentially expressed symbiont genes were identified with the following criteria: adjusted FDR < 0.05 and fold-change > 0.5.

Quantitative PCR

Symbiont plasmid copy number was measured across host compartments by quantitative polymerase chain reaction (qPCR). DNA was extracted from egg caplets, foregut symbiotic organs of larvae and adults using the QIAGEN DNeasy Blood & Tissue Kit with RNase treatment. PCR reactions of 25 µl were set up using the Qiagen SYBR Green Mix using the following parameters: 95°C for 10 min, 45 cycles of 95°C for 30 s, 62.7°C for 20 s, and a melting curve analysis was conducted by increasing temperature from 60 to 95°C during 30 s on an Analytik Jena qTOWER³ cycler. Standard curves (10-fold dilution series from 10⁻¹ to 10⁻⁸ ng µl⁻¹) were generated using purified PCR products. Absolute gene copy numbers were obtained by interpolating the obtained Ct value against the standard curve. Plasmid copy number was determined by dividing the polygalacturonase copy number, localized in plasmids, by the absolute copy number of the chromosomal genes chaperonin GroEL (*groL*) and the 16S rRNA gene.

Long-read sequencing and beetle genome assembly

High molecular weight genomic DNA was extracted from the whole body of four *Calyptocephala attenuata* adults using the Monarch HMW DNA extraction kit for tissue from NEB. The extracted DNA was sheared to between 15 kb and 20 kb using the Megaruptor 2 (Diagenode). A HiFi sequencing library was prepared using SMRTbell Express Template Prep Kit 2.0. Size selection of the final library was performed by the BluePippin System from SAGE Science. Fractions for sequencing were selected based on results from the Femto Pulse System. Desired size fractions were pooled and the final library was purified and concentrated using AMPure PB beads. Quantity of the final library was assessed using the Qubit™ dsDNA HS Assay Kit and the final size distribution was confirmed on the Femto Pulse. Sequencing was performed using one 8M SMRT cell on the PacBio Sequel II System at the Max Planck for Biology (Tübingen, Germany). The pbbccs tool from the pbbioconda package (-min-passes 3 -min-rq 0.99 -min-length 10 -max-length 50000) was utilized to generate the High Fidelity (HiFi) reads (>Q20). Genome assembly was performed by Hifiasm (v0.14.1-r314).¹¹⁹ Polygalacturonase gene identified initially with Illumina sequencing was aligned to the *C. attenuata* draft assembly. Polygalacturonase-containing contigs were extracted and further annotated by AUGUSTUS¹⁰⁸ using *Tribolium* as a training set. PCR targeting this gene in legs, thorax and elytra of *C. attenuata* confirmed that early diverging cassidinae from the Sphillophorini tribe encode a polygalacturonase gene endogenously (PCR primers [key resources table](#)).

Host RNAseq, transcriptome assembly, and CAZy annotation

Internal organs from *Chelobasis bicolor* and *Calyptocephala attenuata* were dissected and snap-frozen in liquid nitrogen. Total RNA was extracted using the QIAGEN RNeasy Mini Kit with DNase treatment. RNA was quantified using the Qubit™ RNA High Sensitivity (HS) kit. 600 ng of total RNA were used as input for RNA sequencing library preparation. mRNA enrichment was performed using the NEBNext® Poly(A) mRNA Magnetic Isolation Module. RNAseq libraries were constructed using the NEBNext® Ultra™ Directional II RNA Library and their size was confirmed in a 2100 Bioanalyzer system using the Agilent Technologies High Sensitivity DNA Kit. Sequencing was performed on an Illumina NextSeq 2000 system at the Max Planck for Biology (Tübingen, Germany) using paired-end chemistry (2x150bp) with a depth of ~40 million reads. Adapters were removed from reads and quality filtered by Trimmomatic.⁸¹ RNAseq reads for *Acromis sparsa*, *Chelymorpha alternans*, *Cassida rubiginosa*, *Parachiridia semiannulata*, *Ischnocodia annulus*, *Cistudinella foveolata*, and *Discomorpha panamensis* were retrieved from NCBI (accession numbers in [Table S1](#) and [key resources table](#)) and included in this comparative analysis. *De novo* transcriptome assemblies for nine cassidines was performed using the Trinity platform (v2.8.5)¹⁰⁹ (--normalize_by_read_set, --SS_lib_type RF). Assemblies were assessed by BUSCO (v5.1.2)¹¹⁰ using the OrthoDB v.10 Enderopterygota gene set¹¹¹ ([Table S1](#)). Protein-coding genes were identified from transcriptome assemblies by TransDecoder (v5.5.0).¹¹² Carbohydrate-active enzymes (CAZs) present were annotated by the dbCAN2 standalone tool run_dbcan4.¹²⁰

Thin layer chromatography (TLC)

Qualitative analysis of breakdown products was performed by thin layer chromatography (TLC) of 20 µl enzyme assays set up as follows: 14 µl of crude gut extract of symbiotic *Chelymorpha alternans* and *Chelobasis bicolor* were incubated with 0.2% polygalacturonic acid in 20 mM citrate/phosphate buffer pH 5.0 at 40°C for 16 h. Polygalacturonase from *Aspergillus niger* was used as a positive control (16 µl of a 0.08 mg/ml solution). Incubated samples were further diluted (1:4) with H₂O and a total of 16 µl were applied to TLC plates (Silica gel 60, 20 × 20 cm, Merck) in 4 µl steps. Plates were ascendingly developed with ethyl acetate:glacial acetic acid:

formic acid:water (9:3:1:4) for about 90 min. After drying, carbohydrates were stained by dipping the plates in a solution containing 0.2% (w/v) orcinol in methanol:sulfuric acid (9:1), followed by a short heating until spots appeared. The reference standard contained 1 $\mu\text{g}/\mu\text{l}$ each of galacturonic, di-galacturonic and tri-galacturonic.

Mannanase activity was qualitatively assessed using 100 μl enzyme assays set up as follows: 40 μl crude gut extract of *Chelymorphism alternans* and *Chelobasis bicolor* were incubated with 0.15% Glucomanan in 30 mM citrate/phosphate buffer pH 6.0 at 70°C for about 1h. Mannanase from *Aspergillus niger* was used as a positive control (1 μl of a 10 $\mu\text{g}/\text{ml}$ solution). A total of 16 μl from each sample were applied to TLC plates (Silica gel 60, 20 \times 20 cm, Merck) in 4 μl steps. Plates were developed ascending with 1-Butanol:glacial acetic acid:water (2:1:1) for about 90 min. After drying, carbohydrates were stained by dipping the plates in a solution containing 0.2% (w/v) orcinol in methanol:sulfuric acid (9:1), followed by a short heating until spots appeared. The reference standard contained 1 $\mu\text{g}/\mu\text{l}$ each of mannose, mannobiose, mannotriose and mannotetraose.

Fluorescence *in situ* hybridization (FISH)

To localize *Stammera* in foregut-symbiotic organs of hispine and tortoise beetle species, as well as in eggs and foregut-symbiotic organs of *C. alternans* larvae and adults, we applied fluorescence *in situ* hybridization (FISH) on paraffin sections. Eggs and foregut-symbiotic organs were dissected and fixed in 4% paraformaldehyde (paraformaldehyde: PBS1X) (v/v) at room temperature during 4h under gentle shaking (500 rpm). After dehydration in an increasing ethanol series of 50, 70, 80, 96 and 100% (v/v) for 1h each, samples were further dehydrated in Roti®-Histol (Carl-Roth, Germany) overnight and embedded in paraffin (Paraplast High Melt, Leica, Germany) overnight. The paraffin-embedded samples were cross-sectioned at 10 μm using a microtome and mounted on poly-L-lysine-coated glass slides (Eprelia, Germany) in a water bath. Paraffin sections were left to dry in vertical position at room temperature overnight and baked at 60°C for tissue adherence improvement. They were dewaxed with Roti®-Histol in three consecutive steps for 10 min each followed by decreasing ethanol series of 100, 96, 80, 70 and 50% (v/v) for 10 min each and then washed in milliQ water for 10 min. Slides were dried at 37°C for 30 min and sections were surrounded by a PAP-pen circle to avoid buffer leaking during hybridization. Foregut-symbiotic organs of Cassidinae beetles were hybridized with the probe SCA600 doubly labeled with the fluorophore Cy5 whereas eggs and foregut-symbiotic organs of *C. alternans* larvae and adults were hybridized with the probe SAL227 doubly labeled with the fluorophore Atto550. The oligonucleotide probe SCA600 was designed to target the 16S rRNA sequence of *Stammera* from 52 cassidines and the SAL227 probe was designed to specifically target the 16S rRNA sequence of *Stammera* from *C. alternans* using the software ARB (99) (key resources table). To target host tissues, the generic eukaryotic probe EUK-1195 (key resources table) doubly labeled with the fluorophore Atto488 was included in both hybridization treatments. All probes were dissolved at 5 ng μl^{-1} in the hybridization buffer containing 35% formamide (v/v), 900 mM NaCl, 20 mM Tris-HCl pH 7.8, 1% blocking reagent for nucleic acids (v/v) (Roche, Switzerland), 0.02 SDS (v/v) and 10% dextran sulfate (w/v). Fifty microliters of hybridization buffer were used per section. The slides were placed in a hybridization chamber at 46°C for 4h with KIMTECHScience precision wipes (Kimberly-Clark, TX, USA) partially soaked in formamide 35% to maintain a humid atmosphere. Sections were rinsed in pre-warmed 48°C washing buffer (70 mM NaCl, 20 mM Tris-HCl pH 7.8, 5 mM EDTA pH 8.0, and 0.01% SDS (v/v)) and transferred to fresh pre-warmed washing buffer for 15 min followed by 20 min in room temperature 1X PBS and 1 min in room temperature milliQ water. After washing, sections were counterstained with DAPI for 10 min at room temperature, dipped in milliQ water, dipped in ethanol 100% and dried at 37°C for 30 min. Slides were mounted using the ProLong® Gold antifade mounting media (Thermo Fisher Scientific, MA, USA), cured overnight at room temperature and stored at -20°C until visualization. Samples were visualized using an LSM 780 confocal microscope (Zeiss, Deutschland). All steps during and after hybridization were done in darkness.

QUANTIFICATION AND STATISTICAL ANALYSIS

All statistical analyses were carried out in R.⁹⁰

Correlation between *Stammera*'s genome size and number of protein-coding genes was evaluated using a Spearman's rank correlation test in R v. 4.3.1.⁹⁰

Species richness and number of host plant families were compared between non-symbiotic and symbiotic cassidines using the G-test of goodness-of-fit.¹¹⁶ As outlined by Edger et al.,¹¹³ G-tests of goodness-of-fit were performed in R v. 4.1.1⁹⁰ using the DescTools package¹²¹ to test if our observed values are significantly different from expectations, assuming equal species in both conditions. A Williams correction was implemented for a better approximation of the chi-square distribution, resulting in a more conservative test.¹¹⁶

To compare the expression of polygalacturonase and α -glucuronidase genes of *Stammera* across host compartments, normalized transcripts were analyzed using a negative binomial generalized linear model implemented by the 'glm.nb' function of the R (4.3.1) package MASS.¹⁰² *Post hoc* Tukey HSD test was performed using the 'glht' function of the R package *multcomp*¹⁰⁷ with Bonferroni corrections.

Differences in plasmid copy number across host compartments were analyzed using a general linear model, after validation of a normal distribution, and using host compartments and replicates as fixed factors. *Post hoc* Tukey HSD test was performed using the 'glht' function of the R package *multcomp* with Bonferroni corrections in R v.4.1.1.⁹⁰

Further statistical details for each test (e.g. exact value of n, meaning of n, precision measures, etc.) can be found in the main text and figure legends. For every statistical analysis significance was defined as a $p < 0.05$.

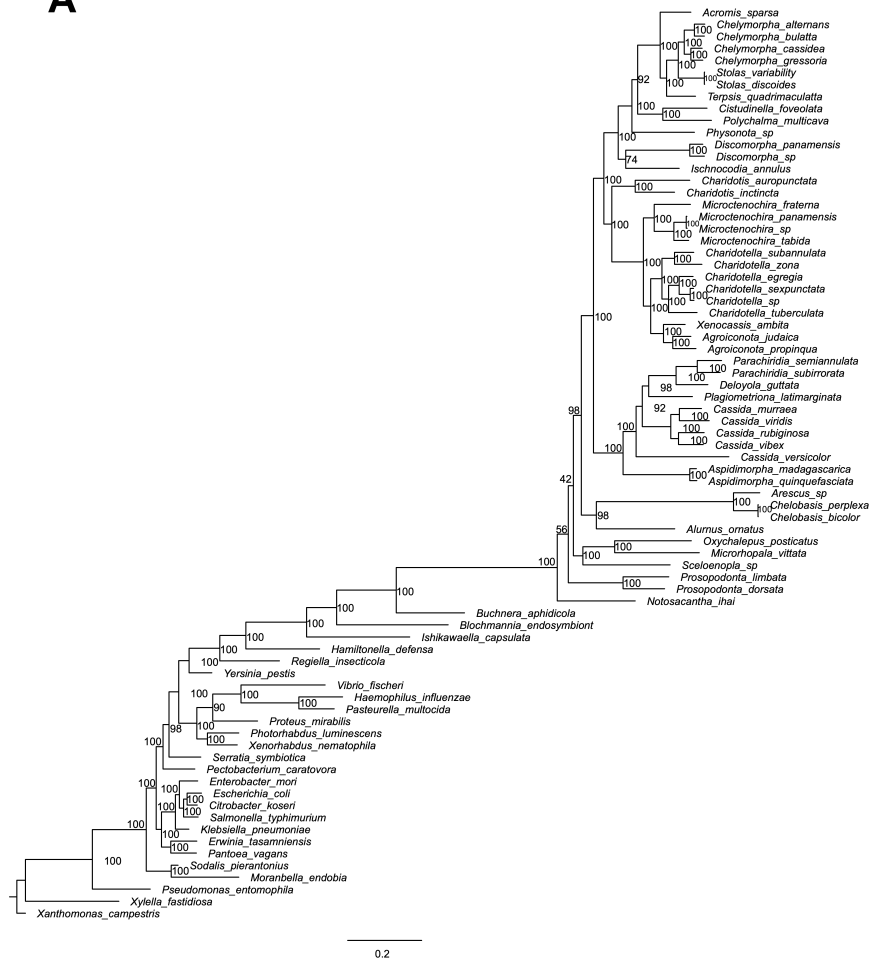
Current Biology, Volume 34

Supplemental Information

Paleocene origin of a streamlined digestive symbiosis in leaf beetles

Marleny García-Lozano, Christine Henzler, Miguel Ángel González Porras, Inès Pons, Aileen Berasategui, Christa Lanz, Heike Budde, Kohei Oguchi, Yu Matsuura, Yannick Pauchet, Shana Goffredi, Takema Fukatsu, Donald Windsor, and Hassan Salem

A



B



Figure S1. Full detailed *Stammera* phylogenies including outgroups based on Bayesian A and Maximum Likelihood methods B, Related to Figure 1

Phylogenomic trees were constructed based on a concatenated alignment of 61 single-copy core genes in MrBayes and RAxML, respectively, using the most appropriate substitution model according to PartitionFinder2. Bayesian posterior probabilities and bootstrap support values are shown for each node. Bacterial genomes used as outgroups were obtained from NCBI and accession numbers are indicated in the STAR Table.

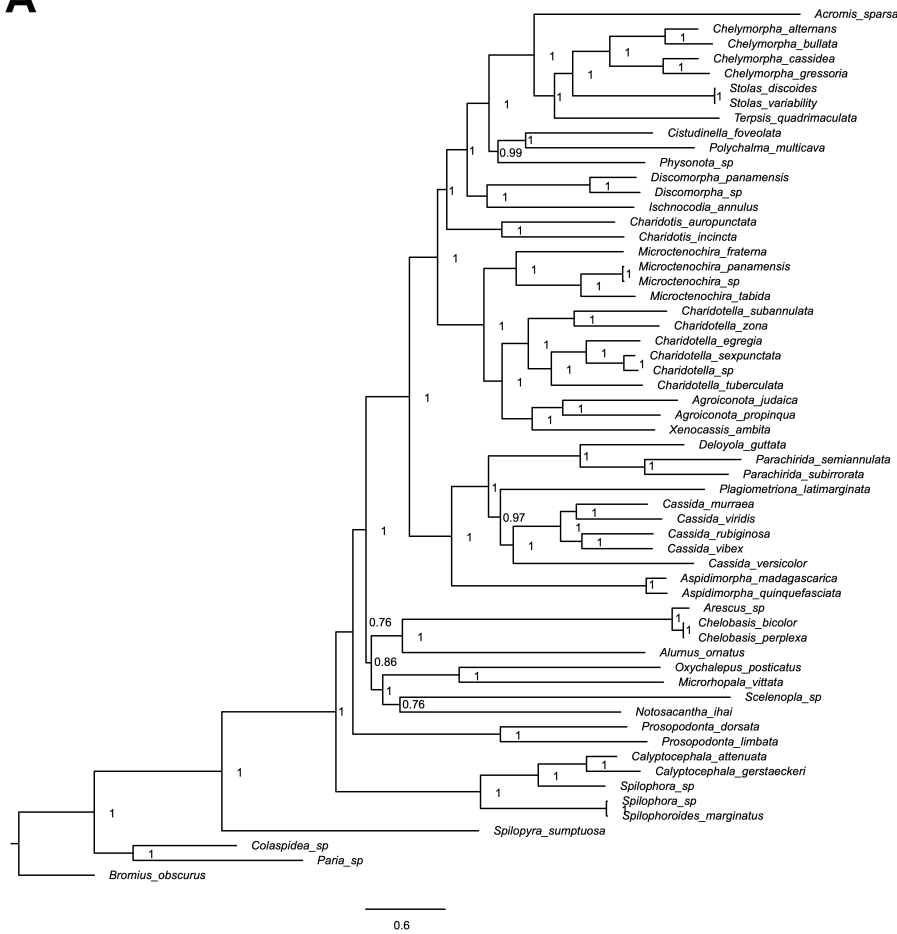
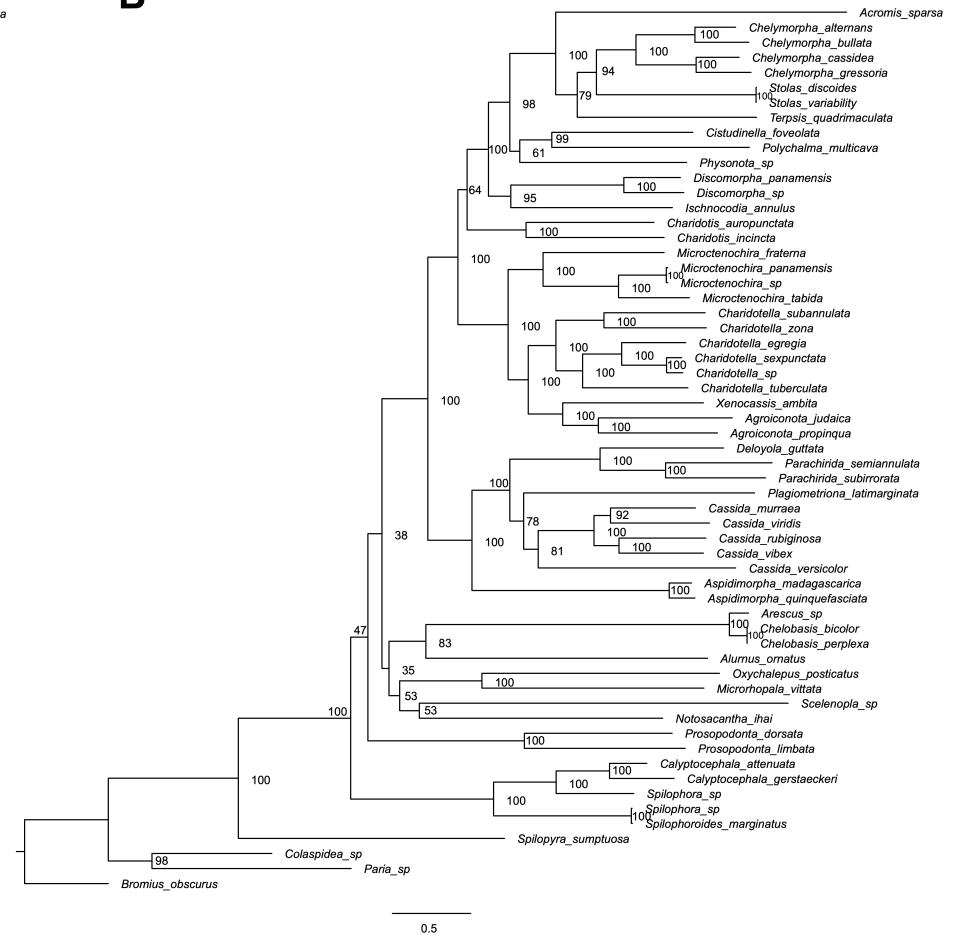
A**B**

Figure S2. Full detailed host phylogenies based on 15 mitochondrial genes, Related to Figure 1

Phylogenetic trees were constructed by Bayesian (A) and Maximum Likelihood (B) methods. Bayesian posterior probabilities and bootstrap support values are shown for each node.

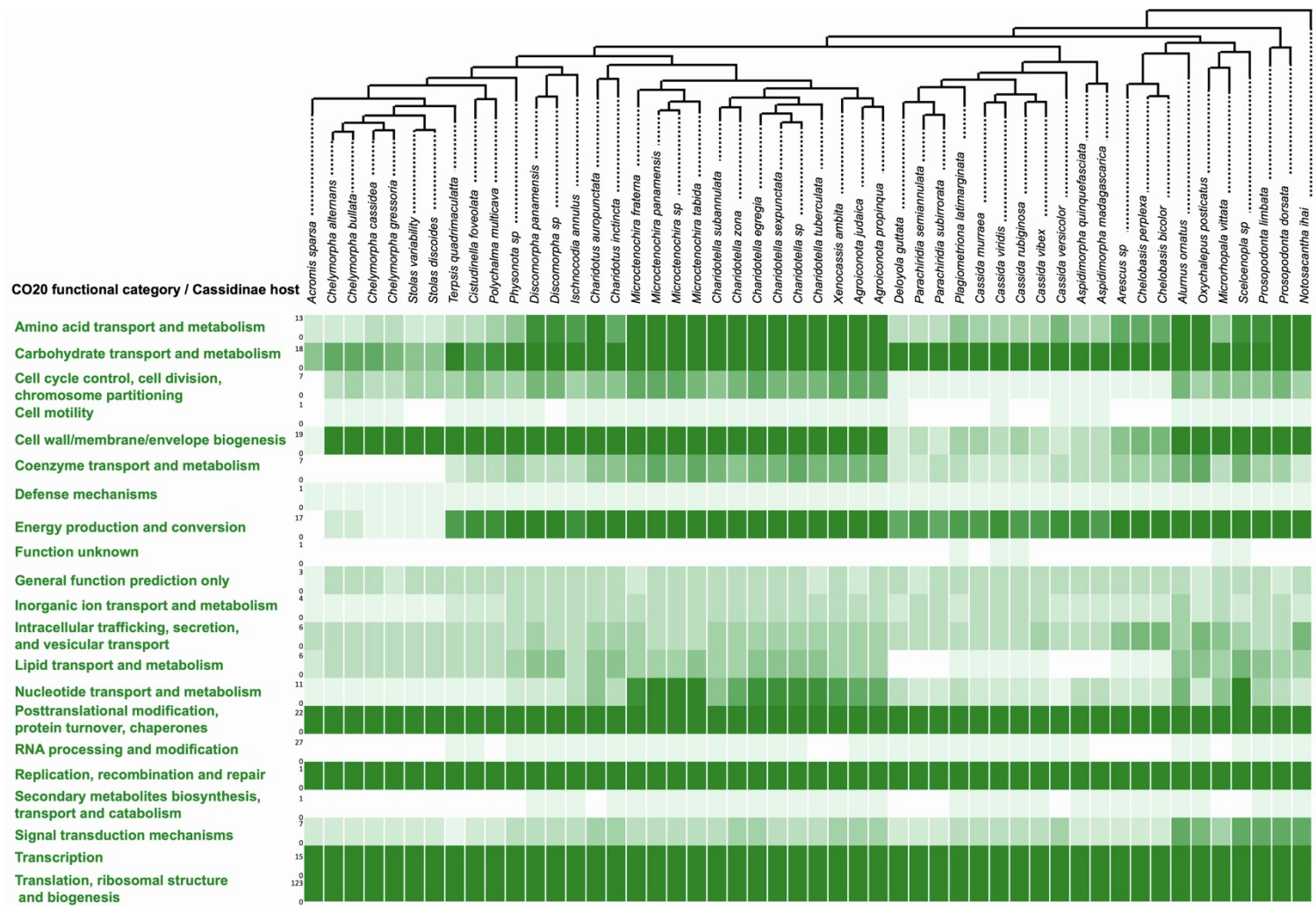
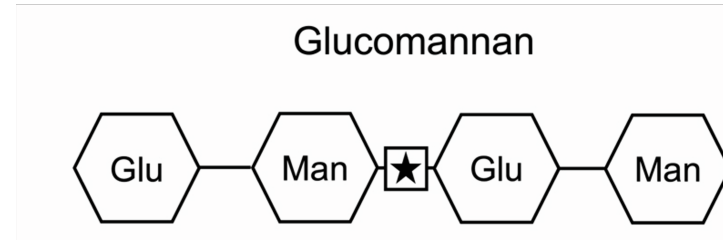
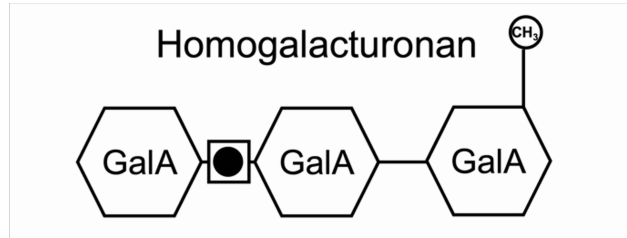
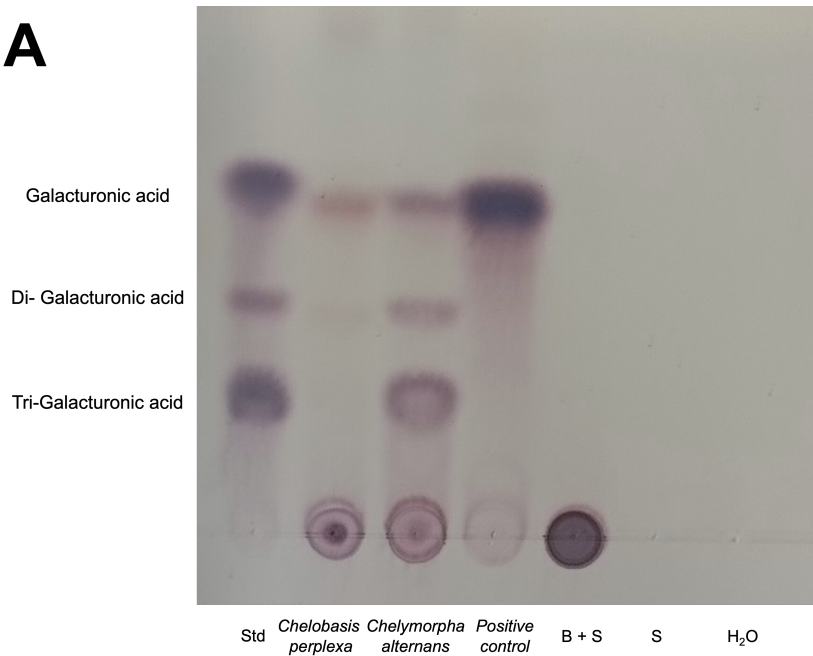


Figure S3. Frequency of Cluster of Orthologous Genes functional categories across *Stammera* genomes, Related to Figure 2

This figure is based on the pangenome obtained comparing gene functions across genomes rather than sequences. Frequency is displayed by an increasing gradient of colors where grey indicates absence of genes belonging to a functional category and dark green indicates the highest gene frequency of a category in a particular *Stammera* genome. The number at the right of the category name indicates the minimum (bottom) and maximum (top) number of genes belonging to that category.



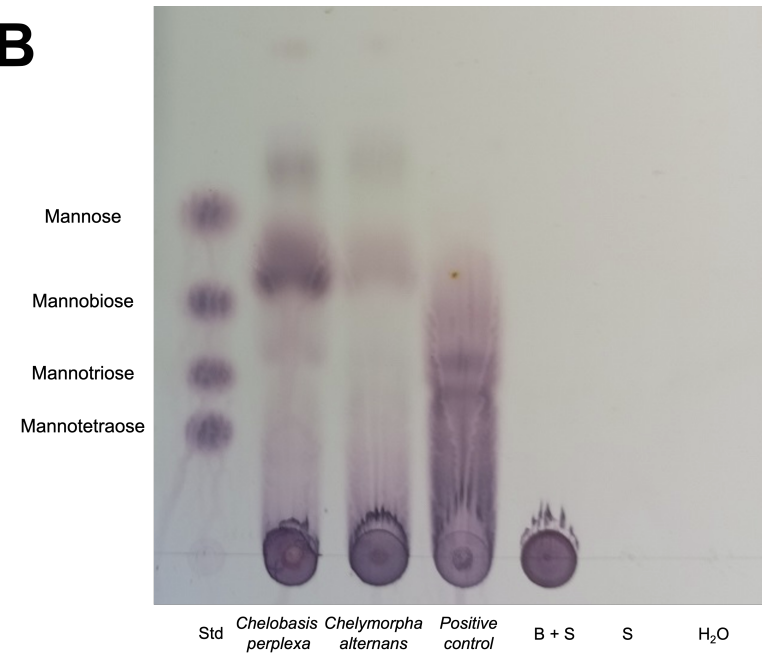
A



Stammera digestive enzymes

Polygalacturonase (GH28) + +

B



Stammera digestive enzymes

Endomannanase (GH5) + -

Figure S4. *Stammera* upgraded the digestive capacity of the hispine beetle *Chelobasis bicolor*, Related to Figure 6

Thin-layer chromatogram (TLC) illustrating the breakdown products of polygalacturonase activity (A) and mannanase activity (B) against polygalacturonic acid and glucomannan, respectively. Gut contents from the hispine beetle *Chelobasis bicolor* and the tortoise beetle *Chelymorpha alternans* were used. Polygalacturonase and mannanase from *Aspergillus niger* were used as positive controls. Abbreviations: B, buffer; S, substrate; Std, standard; GalA, galacturonic acid; Glu, glucose; Man, mannose.

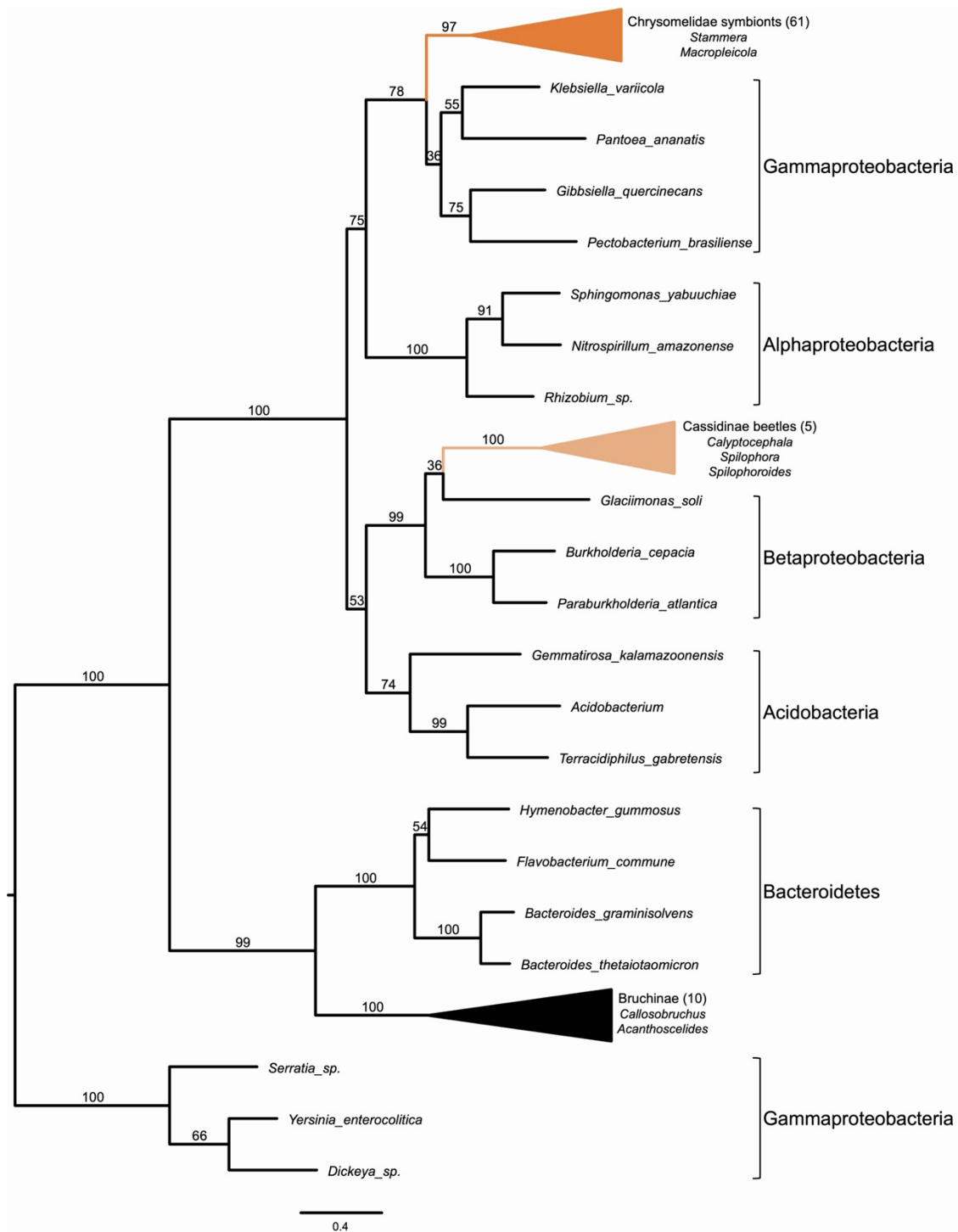


Figure S5. Phylogenetic placement of Cassidinae encoded GH28 pectinases compared to other Chrysomelidae encoded and symbiont encoded GH28s, Related to Figure 6

Maximum Likelihood phylogeny is based on an alignment of protein sequences from Proteobacteria, Bacteroidetes, Bruchinae beetles (black triangle), Chrysomelidae symbionts (dark orange triangle) and non-symbiotic Cassidinae (light orange triangle). Triangles indicate collapsed clades.

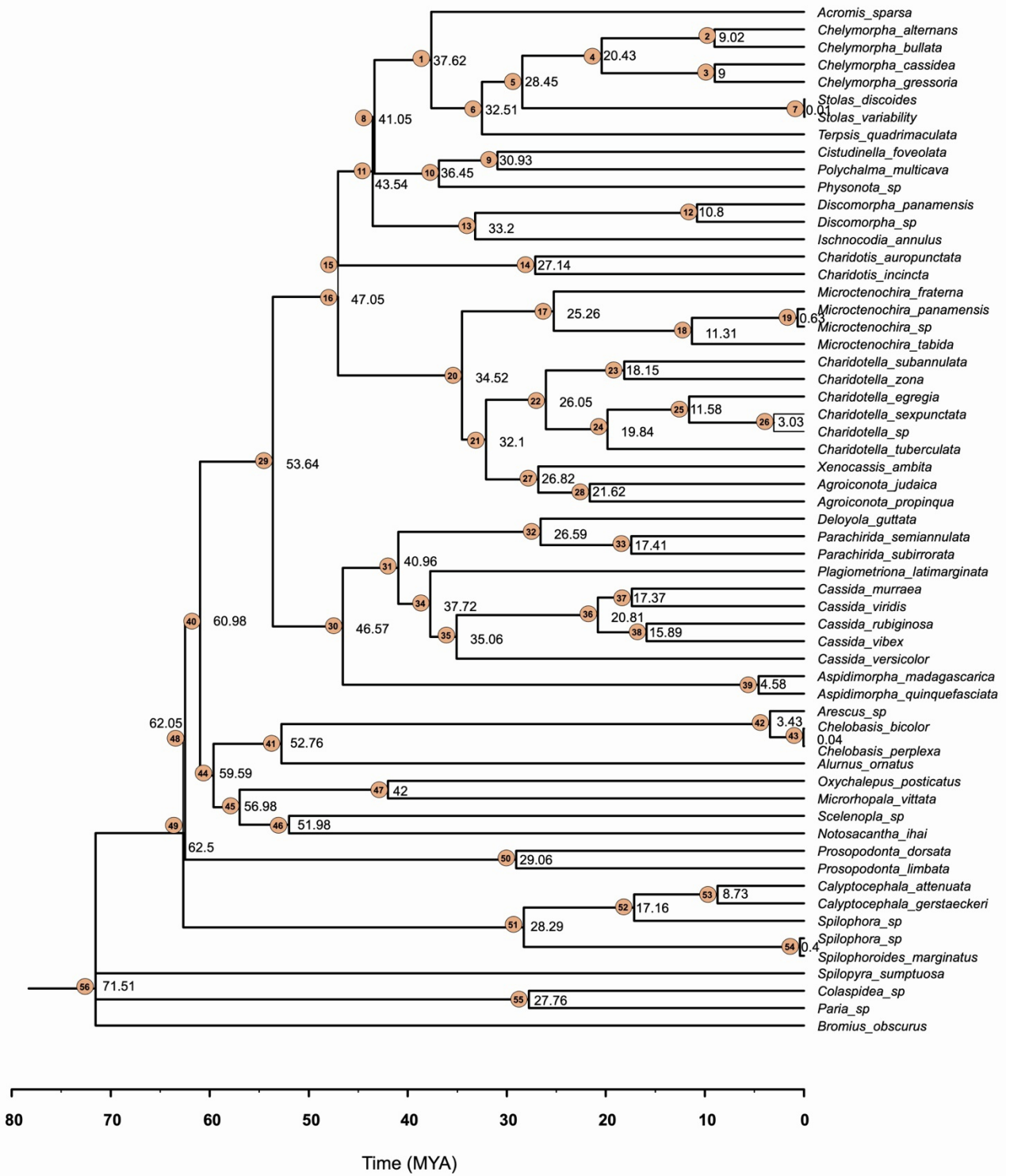


Figure S6. Divergence-date estimates for the Cassidinae based on 15 mitochondrial genes in BEAST analyses, Related to Figure 7 and Table S2

Median date estimates (in million years) are indicated for each node. Intervals for each estimate date are included in Table S2.

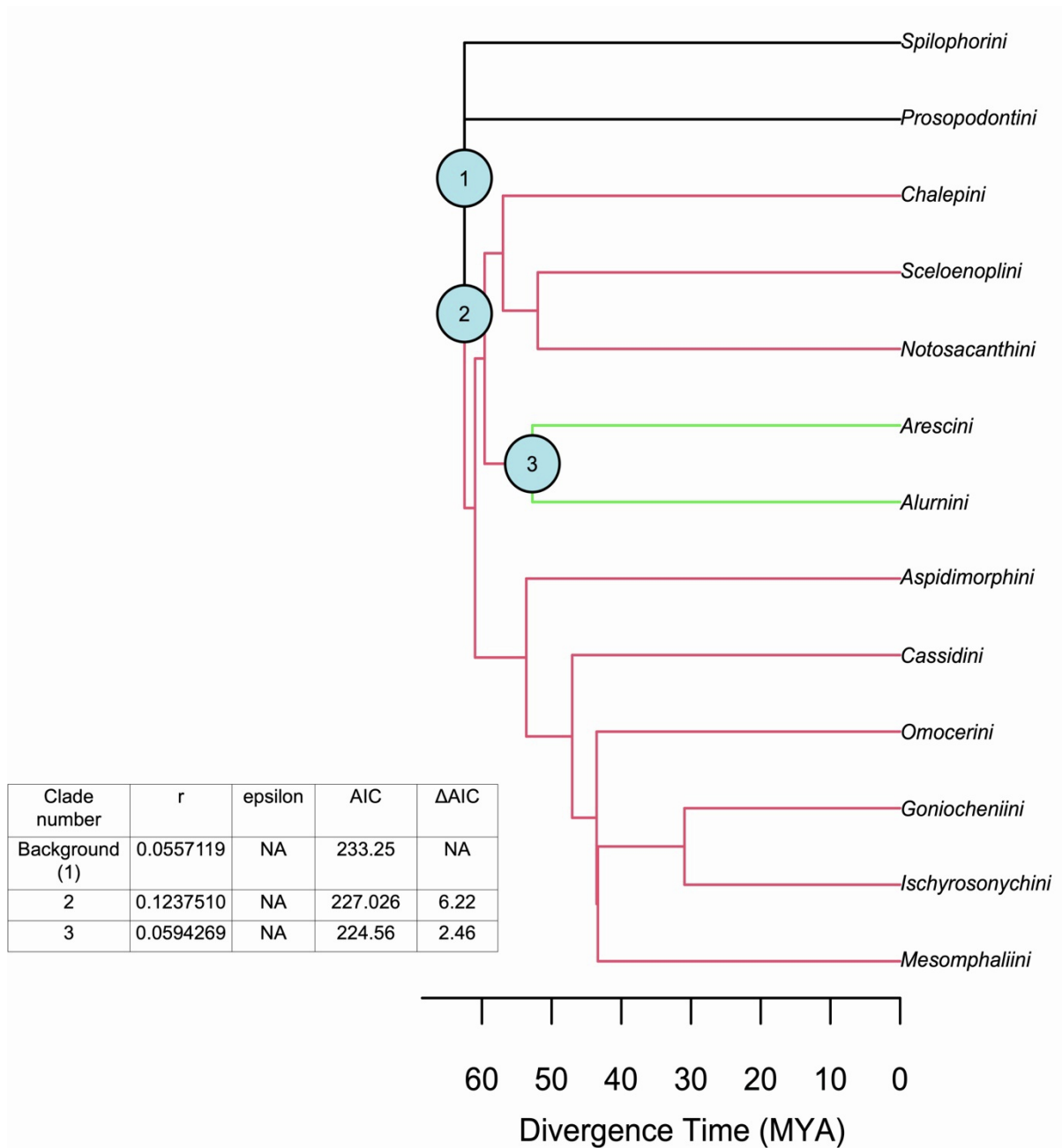


Figure S7. Tribe-level Cassidinae tree indicating the diversification shifts identified by MEDUSA, Related to Figure 7

Branch color indicates an increase (red) or a decrease (green) in diversification across the Cassidinae phylogeny. Clade number included in the table represents the rate shifts identified in the tree. Average diversification rate is indicated by *r*. AIC and Δ AIC show improvement of AIC score over a yule model.

Beetle species	Total assembled bases	Total trinity transcripts	N50	BUSCO (%)	SRA accession numbers
<i>Acromis sparsa</i>	105149650	119737	1659	92,1	SRR10030202
<i>Chelymorpha alternans</i>	91832612	65919	3045	92,6	SRR10030205
<i>Cistudinella foveolata</i>	102002124	99490	1964	92,4	SRR10030206
<i>Discomorpha panamensis</i>	66934931	60044	2037	88,5	SRR10030201
<i>Ischnocodia annulus</i>	80944880	88954	1883	83,1	SRR10030203
<i>Cassida rubiginosa</i>	946549465	1476805	895	94,8	SRR6176960
<i>Parachirida semiannulata</i>	54754341	63170	1605	79,6	SRR10030204
<i>Chelobasis bicolor</i>	100449227	99284	2076	93,9	This study
<i>Calyptocephala attenuata</i>	73049777	86241	1743	89,7	This study

Table S1. Assembly statistics of Cassidinae transcriptomes, Related to Figure 6

Data for *Chelobasis bicolor* and *Calyptocephala attenuata* were generated in this study. Other RNAseq data sets were obtained from a previous study by ^{S1} and Sequence Read Archive (SRA) accession numbers are indicated in the following table.

Node	Median estimate (MYA)	95% Confidence interval
1	37.62	35.43 - 40
2	9.02	8.26 - 9.77
3	9	8.26 - 9.76
4	20.43	19.02 - 21.77
5	28.45	26.63 - 30.21
6	32.51	30.5 - 34.49
7	0.01	0 - 0.02
8	41.05	38.95 - 43.43
9	30.93	28.71 - 33.23
10	36.45	34.03 - 38.67
11	43.54	41.19 - 45.82
12	10.8	9.91 - 11.67
13	33.2	30.7 - 35.69
14	27.14	25.15 - 29.22
16	47.05	44.64 - 49.57
17	25.26	23.55 - 27
18	11.31	10.45 - 12.24
19	0.63	0.53 - 0.74
20	34.52	32.56 - 36.4
21	32.1	30.27 - 33.88
22	26.05	24.39 - 27.59
23	18.15	16.75 - 19.45
24	19.84	18.49 - 21.23
25	11.58	10.68 - 12.46
26	3.03	2.73 - 3.35
27	26.82	25.23 - 28.62
28	21.62	20.12 - 23.16
29	53.64	50.97 - 56.42
30	46.57	44.11 - 49.08
31	40.96	38.83 - 43.1
32	26.59	24.89 - 28.36
33	17.41	16.16 - 18.72
34	37.72	35.61 - 39.79
35	35.06	33.19 - 36.96
36	20.81	19.53 - 22.12
37	17.37	16.14 - 18.68
38	15.89	14.68 - 17.07
39	4.58	4.14 - 5.06
40	60.98	58.06 - 63.96
41	52.76	49.68 - 56.27
42	3.43	3.07 - 3.74
43	0.04	0.02 - 0.06
44	59.59	56.91 - 62.65
45	56.98	54.23 - 59.75
46	51.98	49.68 - 54.33
47	42	39.8 - 44.13
48	62.05	59.99 - 64.34
49	62.5	59.37 - 65.6
50	29.06	26.84 - 31.11
51	28.29	26.37 - 30.23
52	17.16	15.96 - 18.43
53	8.73	8 - 9.47
54	0.4	0.31 - 0.48
55	27.76	25.87 - 29.83
56	71.56	67.6 - 75.36

Table S2. Divergence-date estimates MYA for all the nodes across the Cassidinae obtained from BEAST, Related to Figure 7 and Figure S11

Median estimates and the 95% highest posterior density intervals are included.

Supplemental Reference

- S1. Salem, H., Kirsch, R., Pauchet, Y., Berasategui, A., Fukumori, K., Moriyama, M., Cripps, M., Windsor, D., Fukatsu, T., and Gerardo, N.M. (2020). Symbiont digestive range reflects host plant breadth in herbivorous beetles. *Curr. Biol.* *30*, 2875-2886.e4.